

**Covert Channels in Ad Hoc Networking: An Analysis using the Optimized
Link State Routing Protocol**

by

Jonathan Edwards, B.Sc

A thesis submitted to the Faculty of Graduate and Postdoctoral Affairs

in partial fulfillment of the requirements for the degree of
Master of Applied Science in Electrical and Computer Engineering

Ottawa-Carleton Institute for Electrical and Computer Engineering (OCIECE)

Department of Systems and Computer Engineering

Carleton University

Ottawa, Ontario, Canada, K1S 5B6

April 2012

© Copyright 2012, Jonathan Edwards

The undersigned recommends to
the Faculty of Graduate and Postdoctoral Affairs
acceptance of the thesis

**Covert Channels in Ad Hoc Networking: An Analysis using the Optimized
Link State Routing Protocol**

submitted by

Jonathan Edwards, B.Sc., University of Alberta, 2004

in partial fulfillment of the requirements for
the degree of Master of Applied Science in Electrical and Computer Engineering

Chair, Howard Schwartz, Department of Systems and Computer Engineering

Thesis Co-Supervisor, Peter Mason

Thesis Co-Supervisor, Richard Yu

Carleton University
April, 2012

Abstract

This thesis presents a non-intrusive approach to creating a covert communications channel in Mobile Ad Hoc Networks (MANETs). This is accomplished by manipulating HELLO message timing in the Optimized Link State Routing (OLSR) protocol.

A covert timing channel implementation, requiring no changes to the underlying aspects of the OLSR protocol, is presented. The theoretical channel capacity is derived using information theory. Receiver detection and error control coding methodologies are applied towards maximizing covert channel throughput and minimizing Bit Error Rate (BER). Additionally, previous research efforts in MANET defence mechanisms are expanded, including: detection of wormhole attack and authentication of other nodes.

The theoretical development is re-enforced using simulation including: ns2, MATLAB, Exata and a physical test-bed. It is concluded that receiver detection and error correction can optimize covert channel communication over OLSR; furthermore, it allows for the computation of a simple metric used to detect the presence of a wormhole.

Acknowledgements

I would like to thank my supervisors, Dr. Richard Yu, at Carleton, as well as Dr. Peter Mason and Dr. David Brown at Defence Research and Development Canada (DRDC) for their support, patience and excellent understanding of the vital subject areas of this thesis. I also wish to also thank Dr. Ming Li at DRDC for his support in supplying the relevant hardware and guidance in the experimental phase of this thesis.

Finally, I would like to thank my wife, Ayça, and her family. Without their help this thesis would never have been realized. I dedicate this thesis to my son, Teo.

Table of Contents

Abstract	iii
Acknowledgements	iv
Table of Contents	v
List of Tables	vii
List of Figures	viii
List of Equations	ix
1 Chapter: Introduction	1
1.1 Motivation	2
1.2 Objective.....	4
1.3 Outline.....	5
1.4 Contributions	6
2 Chapter: Background	7
2.1 Mobile Ad hoc Networking	7
2.2 Ad Hoc Protocols and Optimized Link State Routing	8
2.3 Timing Delay Communication with Jitter	10
2.4 Medium Access Control with IEEE 802.11.....	12
2.5 Security Challenges to MANETs.....	14
2.5.1 Wormholes	14
2.5.2 Trust in Sensor Networks	16
2.6 Assumptions and Limitations	18
3 Chapter: The Covert Channel	20
3.1 Modeling the Channel using HELLO Message Traffic.....	20
3.1.1 Communicating with Message Jitter	20
3.1.2 Receiver Noise and Delay	24
3.2 Calculating Channel Capacity.....	26
3.2.1 Capacity of a Noiseless Channel.....	26
3.2.2 Deriving the Capacity of a Noisy Channel.	28
3.2.3 Self Information	28
3.2.4 Entropy	29
3.2.5 Mutual Information	30
3.2.6 Noisy Channel Capacity Calculations.....	31
3.3 Receiver Detection Theory	35
3.3.1 Maximum likelihood Symbol Detection	35
3.3.2 Maximum likelihood Sequence Detection	36
3.3.3 Gray Mapping.....	37
3.3.4 Symbol Reliability with Bit Log-Likelihoods	38
3.4 Improving the Model with Coding Theory.....	40
3.4.1 Block Coding Schemes	41
3.4.2 Convolutional Coding	42
3.5 Complete Covert Channel Systems Perspective.	45

4	Chapter: Covert Channel Evaluation	48
4.1	Measuring Channel Stealth.....	48
4.2	Covert Channel Side Effects.....	50
4.3	Detecting Wormholes through Statistical Methods.....	51
4.4	Wormhole Detection Avoidance Techniques	52
4.5	Review of Alternate Covert Channel Methods	53
5	Chapter: Simulation and Experimental Implementation	56
5.1	NS2.....	56
5.2	Wireshark and Tcpdump	59
5.3	MATLAB and Microsoft Excel	60
5.4	Exata Cyber Emulation.....	62
5.5	OLSRd.....	65
6	Chapter: Results	68
6.1	Modeling the Covert Channel with Ns2	68
6.1.1	Covert Channel Noise Model	68
6.1.2	Measuring Channel Capacity.....	70
6.1.3	System Testing under Variable SNR	72
6.1.4	Evaluating Channel Error Rates.....	74
6.2	Improving the System Through Application of Receiver Detection Theory	78
6.2.1	Maximum likelihood Symbol Detection	78
6.2.2	Gray Mapping.....	78
6.3	Improving the Model with Error Coding Theory	80
6.3.1	Linear Coding Schemes.....	80
6.3.2	Convolutional Coding Schemes.....	86
6.4	Covert Channel Detection.....	89
6.5	Wormhole Detection	93
6.6	Exata Emulation.....	99
6.7	OLSRd Test Bed	101
7	Chapter: Conclusion.....	106
7.1	Summary.....	106
7.2	Contributions	107
7.3	Future work.....	108
	Bibliography or References.....	110

List of Tables

Table 1: Ns2 Observed BER using Simple Binning	74
Table 2: Ns2 SER using Simple Binning.....	75
Table 3: BER using Gray Mapping	79
Table 4: BCH(7,4) Code for N=7 bit Symbols	82
Table 5: BCH(n,k) Codes for N=7-bit Symbols	83
Table 6: BCH(n,k) Codes for N=8-bit Symbols	83
Table 7: BCH(n,k) Codes for N=7-bit Symbols with Wormhole Present.....	85
Table 8: BCH(n,k) Codes for N=8-bit Symbols with Wormhole Present.....	85
Table 9: BCH(7,4) for N=7-bit Symbols, no Wormhole Present and no Gray Mapping ..	85
Table 10: Hard Decision Convolutional Codes with no Wormhole Present	87
Table 11: Soft Decision Convolutional Codes with no Wormhole Present	88
Table 12: Soft and Hard Decision Decoders Compared at R=1/2 codes.....	89
Table 13: Soft and Hard Decision Decoders Compared at R=1/2 codes (Wormhole).....	89
Table 14: Mean Cumulative Error Counts.....	97
Table 15: BCH(7,4) Wormhole Detection Statistics	98
Table 16: Exata BER and SER using Bins	100
Table 17: Exata and Test-bed BER and SER using Bins	105

List of Figures

Figure 1: Simple Binning.....	11
Figure 2: Nodal Representation of a Wormhole	14
Figure 3: Trusted Node Routing.....	18
Figure 4: Covert Channel Mechanism.....	22
Figure 5: Simple Binning with Delay Added.....	24
Figure 6: HELLO Message Sequence Chart.....	25
Figure 7: Wormhole Message Sequence Chart.....	26
Figure 8: Communication over a Noisy Channel.....	31
Figure 9: Discrete Binning with Delay Added.....	32
Figure 10: Semi Discrete Binning with Delay Added.....	33
Figure 11: Gray Mapping Example	37
Figure 12: Bit Log-Likelihood Example	38
Figure 13: Simple Convolutional Encoder and associated Transfer Function.....	43
Figure 14: Sample Trellis Diagram	44
Figure 15: OLSR Covert Channel System.....	46
Figure 16: Exata Wireshark Capture	64
Figure 17: OLSRd Experimental Configuration	66
Figure 18: Interference from External APs on OLSRd Experiment	67
Figure 19: T_A Probability Density Function.....	69
Figure 20: T_A Probability Density Function with Wormhole Present	70
Figure 21: C for various N bit symbols without Wormhole Present	71
Figure 22: C for various N bit symbols with/without Wormhole Present	72
Figure 23: Capacity vs SNR.....	73
Figure 24: BER without and with a Wormhole	80
Figure 25: SER with and without a Wormhole.....	80
Figure 26: Teff vs BCH Code Decode Time	84
Figure 27: Covert Jitter Distribution	90
Figure 28: Discrete Keyed Jitter Example	92
Figure 29: Discrete Jitter Values with Noise T_A	92
Figure 30: Wormhole Detection Statistics	96
Figure 31: Non-wormhole Detection Statistics.....	96
Figure 32: Wormhole Detection Confidence Intervals.....	98
Figure 33: T_A Probability Density Function using Exata.....	100
Figure 34: T_A Probability Density Function using OLSRd.....	102
Figure 35: T_A Probability Density Function using OLSRd in Noiseless Environment ...	103
Figure 36: T_A Probability Density Function using Exata and Test-Bed	104

List of Equations

Equation 1: HELLO Message Interval	9
Equation 2: TC Message Interval.....	10
Equation 3: OLSR Message Interval.....	21
Equation 4: HELLO Message Covert Channel Calculation	23
Equation 5: T_A Calculation with the presence of a wormhole	25
Equation 6: Capacity of a Discrete Noiseless Channel	27
Equation 7: Modified Discrete Noiseless Channel Capacity	27
Equation 8: Channel Quantization	27
Equation 9: Self Information.....	29
Equation 10: Entropy of a Random Variable.....	29
Equation 11: Mutual Information of Two Events	30
Equation 12: Average Mutual Information of Two Random Variables	31
Equation 13: Discrete Capacity over a Noisy Channel	31
Equation 14: Semi-Discrete Capacity over a Noisy Channel	33
Equation 15: Approximation of Total Probability	34
Equation 16: Continuous Capacity over a Noisy Channel	34
Equation 17: SNR of Discrete Channel.....	35
Equation 18: Maximum likelihood Symbol Detection.....	35
Equation 19: Maximum Likelihood Sequence Detection.....	36
Equation 20: Log-Likelihood Ratio for bit, B_j	39
Equation 21: Log-Likelihood Ratio for bit, B_j of the Covert Channel	39
Equation 22: Bit Log-Likelihood Example B_1	40
Equation 23: Bit Log-Likelihood Example B_2	40
Equation 24: Block Coding Generator Matrix	41
Equation 25: Minimum Hamming Code Distances	42
Equation 26: Kolmogorov-Smirnov Test Notation	48
Equation 27: Throughput	76
Equation 28: Effective Throughput.....	81

1 Chapter: Introduction

An ad hoc networking is a network of multiple nodes that operate without centralized coordination [1]. Nodes can be mobile and join, leave, and re-join the network. Decisions, such as routing and association, are managed by the nodes independently. However, increased mobility and decentralized control comes at a cost to system security in terms of confidentiality, integrity and availability of communications.

Covert communication is defined here as a method of communication where information passed between entities is undetected and unknown to a third party. Such a method is invaluable for passing information confidentially. In an environment where communication is over-the-air and easily visible to multiple parties, applications that are covert can facilitate secure and reliable communication.

This chapter introduces the motivation, objectives and original contributions of this thesis. This thesis presents an application of error correction coding theory to a covert channel in an ad hoc networked environment using the Optimized Link State Routing (OLSR) protocol. It also presents specific threats, such as “wormhole” replay attacks, which can be detected using the proposed covert channel coding solution. The channel is further parameterized in terms of its theoretical capacity and improvements in reliability over previous models.

1.1 Motivation

Mobile ad hoc networking applications are well suited for environments that are highly dynamic, such as mesh networks. Nodes in these networks handle not only their own traffic but also the traffic of other nodes that use them as intermediary links. This allows traffic to traverse larger distances, provided a sufficient path of linked nodes exists. Advantages of MANETs over a centralized control paradigm can be seen from their inherent redundancy as there is not always a single point of failure in the system. Ad-hoc networks are able to “self-heal” when a node is removed and do not rely on the presence of a central entity to maintain their routing configuration for them.

Military applications are well suited to ad hoc networks given that military or emergency operations require the rapid and mobile deployment of networked assets where the topology is dynamic. In a multi-group collaborative environment, different units, often represented by different groups, come together under a unified structure. In these collaborative group environments the sharing of a common, networked infrastructure is a basic necessity. In such a scenario it may be required by one sub-group to identify its specific nodes or pass information in a covert fashion unbeknownst to the rest of the group. Simply employing encryption between nodes will inform the entire networked group that private communication is taking place.

Consider a set of networked nodes whose traffic is visible by an external observer. When an event takes place the observer is able to observe the details of the event by observing the contents of the traffic passed between nodes. With encryption, confidentiality of the traffic is ensured as the observer can no longer observe the details of the event, but by simply observing the encrypted traffic the observer can infer the

occurrence of an event. With covert communication between the nodes the observer can neither observe the details of the event nor infer its existence. Also, by effectively utilizing such a mechanism, it can be ensured that other potential adversaries are not using the covert channel on the same nodes.

Covert communication could become an avenue for authentication of specific nodes operating within a shared network. By covertly communicating specific credentials, nodes could identify each other or act differently towards authenticated nodes than towards non-authenticated nodes without presenting an easily visible bias. Similarly, private key distribution over such a scheme along with emergency covert broadcast traffic alerting only a subset of nodes becomes possible.

Another major security challenge faced by mobile ad hoc networks is the wormhole attack. Introduced in [2], wormholes have the potential to disrupt or degrade the efficiency of the network by replaying traffic between nodes in an effort to subvert traffic and distort nodes' routing tables. Multiple solutions have been proposed, some of which are examined in this thesis. This thesis proposes new mechanisms to detect the presence of wormholes on ad hoc nodes through a natural application of the covert channel. A node that identifies a wormhole can then adjust its routing tables to ensure traffic is not hijacked and that traffic proceeds to the next legitimate node whereby similar mechanisms can provide the same effect and so on as a means to ensure high availability in a potentially unfriendly environment.

1.2 Objective

This thesis builds on previous methods of wormhole detection [3] and presents a mechanism aimed at improving covert channel communication between ad hoc nodes within the confines of the OLSR routing protocol as defined in RFC 3626 [4]. The objective is to maximize covert channel communication throughput, minimize error rates and improve wormhole detection in the network. The seemingly distinct goals of improving error rates and detecting wormholes are accomplished simultaneously by applying error correction codes to a covert channel and comparing the bit error rates against statistical expectations in various levels of noise, where increased noise (and hence an increased bit error rate) suggests a wormhole may be present.

The central idea of the covert channel is to use a fundamental aspect of the OLSR protocol HELLO message traffic, known as message jitter. Jitter is a small random delay generated by each ad hoc node that is normally used to ensure multiple nodes do not transmit their message traffic at the same time during the broadcast of neighbor discovery information in the form of HELLO messages. Instead of simply generating a random jitter delay, this thesis expands the concept, originally discussed in [3] [5], of keying the jitter with a cryptographic function to pass a covert message, via “random-like” jitter delay timings defined herein as “keyed jitter”. Given that in a real system there will be an element of noise still inherent in the covert channel (i.e., uncontrolled delays in messaging) this thesis examines methods of receiver detection and error correction coding to reduce the effects of noise and simultaneously provides a metric to detect network attacks.

1.3 Outline

In [3] and [5], a method for covert communication that uses timing characteristics of the OLSR protocol was suggested as a potential future area of study. The proposals from [3][5] are extended towards a more robust paradigm using coding theory in addition to addressing concepts of security.

This thesis begins with a relevant description of the technical background of ad hoc networks and current threats in Chapter 2, as well as assumptions made in this thesis.

Chapter 3 introduces the operating premise of the covert channel using the OLSR protocol with emphasis on the relevant aspects to this study and without any required changes to the OLSR protocol. Theory concerning channel capacity is applied and discussed in the context of the OLSR covert timing channel. The improvements in channel throughput and reliability from the use of error correction coding and receiver detection theory are examined against measured SNR and evaluated against the theoretical maximum of capacity as determined by Shannon's equations, for point to point connections.

Chapter 4 presents a criterion for evaluating how difficult it is to detect the presence of the covert channel. It also considers similar covert channel methods and possible advantages of using error correctional coding to detect the presence of wormhole traffic.

Chapter 5 discusses the testing and evaluation aspects of this study in terms of configuration and setup for simulation, emulation and test-bed scenarios.

The results, presented in Chapter 6, demonstrate the ability to reduce covert channel error rates through the adoption of coding theory to the proposed channel.

Different coding methods are compared in terms of their effects on channel throughput and reliability as well as their ability to be used for wormhole detection.

Chapter 7 concludes with the important highlights of the study reiterating the contributions presented here.

1.4 Contributions

The following are the contributions of this thesis in bulleted form for clarity and distinction:

1. This thesis derives the capacity of the covert channel, from [3] [5], and proves that covert channel capacity can be used to quantitatively detect the presence of a network attack via a wormhole.
2. It introduces techniques to enhance the reliability (i.e., reduce the bit error rate) of the covert channel and demonstrate the effectiveness of these techniques, through extensive simulation, while providing guidance on how to maximize the throughput with tradeoffs towards the reliability of the channel.
3. It examines methods of ensuring high assurance covert communications and evaluates the degree to which the proposed timing channel is truly “covert”.
4. Finally, it shows quantitatively, through simulation, that it is possible to improve network attack detection by observing the performance of the error control codes derived from the techniques employed in this thesis. It is shown that the number of errors corrected by the receiver represents a reliable metric for determining the presence of a wormhole.

2 Chapter: Background

This chapter presents the relevant background in mobile ad hoc networking as well as current and prominent threats in mobile ad hoc networking.

2.1 Mobile Ad hoc Networking

Ad hoc networking represents an adaptive solution to a mobile environment where nodes in the network are neither fixed in time nor place. The two most distinctive attributes of an ad hoc network are multi-hop relaying and decentralized control. Multi-hop relaying requires that each node in the network can act as a potential pathway between two or more other communicating nodes that are out of range of each other. Decentralized control means that ad hoc networks function without the requirement for centralized coordination and operate in a distributed fashion whereby each node acts independently. This allows for a more robust and fault tolerant design, but comes with additional overhead as each node must maintain network topology and routing information.

As the topology of all nodes is ever changing, ad hoc routing protocols, are employed to provide a map from one point to another in the network. These protocols must continuously update their routes, either reactively or proactively, as discussed in Section 2.2. The operation of ad hoc networks, including the routing protocols, has been formalized by a working group within Internet Engineering Task Force (IETF) known as the MANET Working Group as presented in [6].

Typical environments where mobile ad hoc networks offer advantages are in environments that require dynamic, scalable and mobile infrastructure. This is true particularly within the military domain, or organizations involved in emergency

operations using sensor networks. The next section discusses the types of routing protocols that operate in these environments.

2.2 Ad Hoc Protocols and Optimized Link State Routing

Ad hoc network protocols can be organized by their route update mechanism, which is either considered to be table-driven (proactive) or on-demand (reactive).

Nodes using reactive routing schemes, such as Ad Hoc On-demand Distance Vector (AODV) routing as defined in IETF RFC 3561¹, determine the route from source to destination on an as-required basis. Another implementation of covert channels over ad hoc networking exists in [7][8] using the AODV protocol and is contrasted to this study in Section 4.5.

Nodes using proactive protocols, which include OLSR, keep network topology and route information in table format. Generally, the table includes the next node to take in a path to a particular destination and the expected distance between them. In order to maintain an accurate picture of the network topology, nodes must exchange routing update information at the cost of additional overhead traffic compared to reactive protocols. The advantage being that at transmission time the node can simply send a packet as opposed to having to seek out routing information. Both proactive and reactive routing protocols both offer unique advantages to the particular environment for which they are best suited.

OLSR extends the methodology of proactive routing protocols by offering a mitigation against the aforementioned route table update overhead by selecting specific nodes, known as multipoint relays (MPRs), to handle packet forwarding and link state

¹ C. Perkins, E. Belding-Royer, and S. Das, "Ad hoc on demand distance vector (AODV) routing," RFC 3561, July 2003.

update forwarding. By having fewer nodes responsible for this task, less data transmission overhead is consumed, resulting in a savings for larger node densities [6]. The OLSR protocol operates by transmitting packets using the user datagram protocol (UDP). Two message types are involved in passing route information in OLSR: the HELLO message and the Topology Control (TC) message. The purpose of HELLO message traffic is to relay neighbor state information, including: link state information and a list of neighbors that have communicated with the node in the past.

HELLO messages can be sent in a jitter-periodic or HELLO-periodic fashion as defined in [4] using Equation 1. Jitter-periodic implementations of OLSR define HELLO message intervals based on when the last message was sent, including its jitter offset. HELLO-periodic defines the intervals, using Equation 1, but is based on the fixed HELLO_INTERVAL where jitter is subtracted each time. This thesis uses the HELLO-periodic approach.

$$\textit{Hello Message Interval}[i] = \text{HELLO_INTERVAL} - \textit{jitter}[i]$$

Equation 1: HELLO Message Interval

The HELLO_INTERVAL is periodic every two seconds. The value of *jitter* from Equation 1 varies with each successive calculation of the *Hello Message Interval* with a range from [0, MAXJITTER], where MAXJITTER is HELLO_INTERVAL/4 or 0.5 seconds as HELLO_INTERVAL is 2 seconds as per [4]. Its intended purpose is to ensure that if multiple nodes are transmitting, the transmit times are randomized in order to prevent collisions from nodes transmitting at the same time. This is accomplished by subtracting a small known random delay, known as jitter, from the HELLO_INTERVAL.

The second type of message worth consideration is the TC message. Its purpose is to relay topology information used to build routing tables. As per [4] the TC interval is

defined by Equation 2 . The TC_INTERVAL is five seconds with an additional known jitter delay of the same range as the HELLO message case.

$$TC\ Interval[i] = TC_INTERVAL - jitter[i]$$

Equation 2: TC Message Interval

Adjacent nodes which receive HELLO and TC Messages will process them, but only nodes selected as MPRs will forward them. For the purposes of covert channel communication the jitter values in both messages can be manipulated to pass a message undetected, but HELLO message traffic is better suited to this purpose due to its smaller interval time, thus offering a higher capacity. As well, since the HELLO message is never forwarded compared to the TC message, there is less confusion around accounting for multi-hop delays [3].

2.3 Timing Delay Communication with Jitter

Given the brief introduction on the purpose of HELLO message jitter, this section offers a brief background on how such jitter can be used to convey a covert message. As introduced in [3] [5] it is possible to introduce deliberate delays (as opposed to random jitter) on the arrivals of HELLO message traffic between adjacent nodes to convey information. This is known as a covert timing channel, where information symbols are represented by the time delay between successive legitimate traffic messages. For example if a HELLO message arrives at (HELLO_INTERVAL – 0.1s) this represents the letter “A” and if it arrives at (HELLO_INTERVAL – 0.15s) it represents “B” and so on. This thesis is concerned with binary communication so the symbols represent binary data, thus the channel must be quantized into 2^N possible values where N is a positive integer. In order for the receiver to determine which symbol was sent the process of “binning” is used as illustrated in Figure 1.

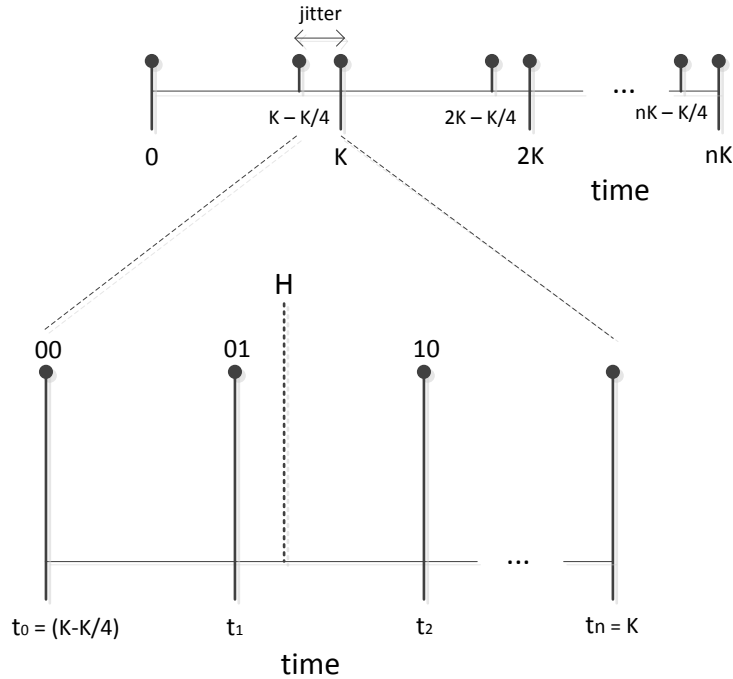


Figure 1: Simple Binning

As illustrated in Figure 1 the x-axis shows the time at which a standard HELLO message, H , is received between the expected minimum and maximum HELLO message interval values, from Equation 1. For example, in the “zoomed-in” portion of Figure 1, as the HELLO message, H , is received closer to the symbol value 01 at t_1 , it can be inferred that the covert message 01 was most likely sent. The covert message symbols are mapped to timing delay values of t and defined based on the channel quantization. As the amount of channel quantization increases, more information can be sent over the channel per HELLO message interval; however the channel is also more susceptible to errors in this case. These concepts are further explored in Chapter 3.

2.4 Medium Access Control with IEEE 802.11

As this thesis is concerned with encoding information in observed message delay, an understanding of the underlying link layer responsible for message passing is required as pertaining to the Medium Access Control (MAC) sub-layer defined by IEEE 802.11 [9].

Multiple different types of MAC protocols exist or have been proposed for ad hoc networking, with 802.11 being one of the most prominent adopted standards. The larger market share of 802.11 devices offers greater relevance to this study as well as a larger comparative base of literature from which to evaluate the results of a covert channel over 802.11.

802.11 MAC uses Carrier Sense Multiple Access with Collision Avoidance (CSMA/CA) in order to determine when a node should transmit on the shared channel. If a node wants to send data, it first listens to the channel and starts sending a frame if the channel is not busy. Should the channel be busy, the sender waits a random transmitter assigned contention back-off period defined as a random multiple of $20\mu\text{s}$ slot sizes after which re-transmission is attempted.

802.11 MAC operates, generally, in either one of two modes: either a distributed coordination function (DCF) mode or a point coordination function (PCF) mode. The difference between a PCF and DCF is the absence of a centralized coordinator in a DCF. A PCF system usually applies to current home 802.11 wireless access using an Access Point as a PCF to coordinate traffic amongst nodes. A DCF system usually uses CSMA/CA to determine when to send messages in the absence of a PCF. Messages that are transmitted must also adhere to specific Inter Frame Spacing (IFS) requirements.

Control messages can wait either short-IFS (SIFS), or a DCF-IFS (DIFS) with delays that vary with priority or depending upon physical layer characteristics, such as the choice of modulation. The reader is encouraged to examine the 802.11 IEEE standards [9] for more detail.

A DCF is the mode modeled in this thesis in regards to the simulation, emulation and test-bed scenarios. Under high traffic environments, the delay experienced by a node waiting to send a message is expected to become larger due to collisions and back off. Constant collisions between nodes transmitting HELLO message traffic results in a more unpredictable HELLO message interval. Since the approach in this thesis uses the HELLO message timing as a means of covert communication, as explained briefly in Section 2.3 and further detailed in Chapter 3, any increased variation in HELLO message arrival leads to channel noise and could contribute to an increased Bit Error Rate (BER) of the covert channel studied in this thesis.

Propagation delay between nodes is significantly smaller (i.e 300ns for a 100m link) than delays caused by collision and back off, and is considered negligible for this thesis. A fully documented study of HELLO message propagation delays is presented in [3]. This thesis will attempt to quantify these delays under specific conditions and will use error correction coding decisions to improve HELLO message covert channels mentioned in [3] [5].

2.5 Security Challenges to MANETs

This section briefly introduces the prominent threats inherent in mobile ad hoc networking which can vastly affect performance or represent security risks.

2.5.1 Wormholes

The wormhole attack, as applied to ad hoc networks, is first introduced in [2] and described using Figure 2.

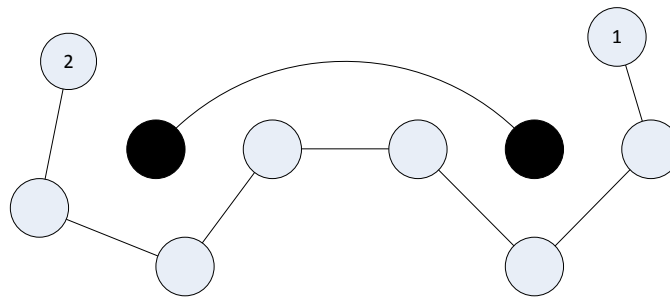


Figure 2: Nodal Representation of a Wormhole

In this figure the light colored nodes represent legitimate nodes. In the functioning of normal OLSR protocol operations these light colored nodes would transmit HELLO messages allowing the nodes to identify their neighbors and generate applicable routing table and topology information. Should Node 1 need to send traffic to Node 2 a potential path is identified, shown using the connected lines between the light colored nodes in Figure 2, consisting of multiple hops through the network.

With the introduction of a wormhole, depicted by the black nodes, it becomes possible to disrupt the topology. These nodes do not act as members of the topology and therefore do not transmit legitimate message traffic or appear as members of the network, but rather passively receive and forward all traffic, known as tunneling. This is explicitly accomplished by the wormhole nodes transmitting between each other on an off-channel

link and then re-broadcasting. The effect is that instead of the path depicted in Figure 2, it will appear that Node 1 and Node 2 are next to each other and their routing topologies will be updated as such. As all the nodes on the left and right side of the diagram, by the means of the wormhole, appear right next to each other. They will fail to seek new routing information and will transmit all traffic through the wormhole.

There are multiple consequences of wormhole manipulation. First, as traffic is now routed through the wormhole, the topology is lost, as inspection of the routing tables demonstrates that distant nodes are in proximity of each other. The wormhole channel can now function as a Man-In-The-Middle (MITM) attack and alter traffic at will, opening up a host of malicious possibilities. Once the wormhole channel is removed all routing topology needs to be reset causing a temporary denial of service.

As proposed in [2] one defense against wormholes uses the concept of “Packet leashing” whereby the node’s known location is used to predict wormhole presence. Another method uses direction finding equipment to predict wormholes, as in [10]. Other approaches exist around modification to the OLSR protocol, as discussed in [11], through the addition of modified HELLO message types targeted at using a timing analysis of HELLO message packet delivery. New algorithms are also proposed in [12] [13] [14] offering unique and effective approaches to wormhole detection at the expense of changes to the underlying OLSR protocol or additional constraints on neighboring nodes in terms of synchronization.

The approach taken in this thesis, through the use of the covert channel, differs from the aforementioned approaches in that it retains compatibility with the original OLSR protocol and does not require any changes to message type or overarching

protocol structure. The work discussed extends that of [15] [16] using packet timing statistics, bit error rate (BER) and tracking corrected errors from channel encoding as additional predictors of wormhole attack in a system of nodes. All the processing required to detect wormhole channels can be implemented within the node internally without changes to the functionality of the protocol, thus maintaining compatibility with unmodified nodes.

2.5.2 Trust in Sensor Networks

Trust plays an important role in any ad hoc network, where any node can join or act as a message forwarding intermediary. In a secure environment, it becomes particularly important to ensure the integrity and authenticity of nodes operating in an ad hoc environment. The OLSR protocol is defined on principles based on a complete trust of neighboring nodes without applicable security controls inherent in its design. In one sense this makes the protocol simple to implement and allows for interoperability between nodes using open standards, yet adds a degree of risk from a security perspective as this exposes the network to potential attack.

As discussed in [17], there exist multiple vectors of attack in ad hoc networks. Network attacks through wormholes as previously discussed are possible. Should the wormhole decide to drop all packet traffic it then becomes a so called “Black hole”. Attacks where malicious nodes are introduced to the network are possible as well. Specific attacks include the fabrication of false routing information used to disrupt the topology and routing tables of cooperative nodes, along with impersonation of nodes acting on behalf of legitimate nodes for nefarious purposes.

Traditional approaches towards the active attacks utilize principles of cryptography [17] to build trust models between nodes, but this is done at either a cost to overall capacity or additional changes to the OLSR protocol [18] [19], among others. The goal of this thesis is to maintain interoperability with partner organizations or cooperative environments sharing nodes in a network where it may not be possible to share security details. The covert channel proposed in this thesis offers a potential mechanism of allowing for authentication of nodes and mitigation of fabricated or “replay attacks” from suspicious nodes through its use.

Trusted nodes can authenticate each other through covert traffic while maintaining interoperability with existing nodes on the network. Depending on the topology, decisions can be taken by each node to use routes through trusted nodes (instead of potentially faster routes) or over un-trusted nodes in specific situations. This is depicted in Figure 3 where the light colored nodes represent trusted nodes authenticated through covert messages. In this example, a routing path is present between only trusted nodes connected by solid lines, which can be used to ensure trusted message delivery. Interoperability between light and dark colored nodes exists, but can be elected to be handled differently by the trusted nodes as required without impact to the basic operating principals of the OLSR protocol. It is noted that keyed jitter can only maintain the authenticity of HELLO messages as used to identify friendly nodes and pass covert messages between them, and not the authenticity of non-covert transmitted traffic, which is still subject to over-the-air attack. Additionally, should replayed or fabricated traffic contain HELLO messages without appropriately keyed jitter, this can serve as a signature for potentially malicious traffic.

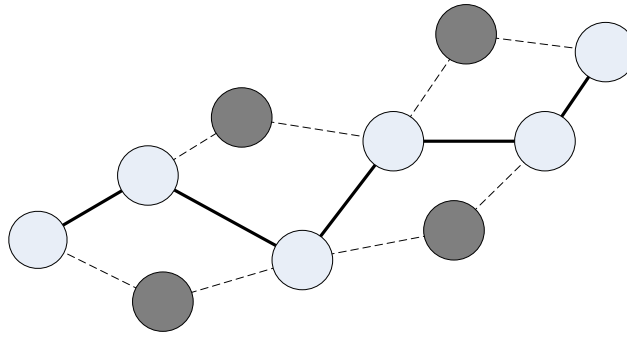


Figure 3: Trusted Node Routing

A particular application of a covert channel may exist in authentication in sensor MANETs where large sets of nodes are deployed. Authentication over a covert channel could offer a means to establish trust throughout the network. This approach guards against false sensors potentially placed in the network to obscure data retrieval or disrupt functionality.

2.6 Assumptions and Limitations

In order to focus on specific aspects of covert message traffic over the OLSR protocol it becomes necessary to make reasonable assumptions of the underlying traffic channels and hardware.

As discussed in further detail in Chapter 3, cryptographically keyed jitter is added to HELLO messages when creating the covert channel. These cryptographic pseudorandom generators are utilized in order to preserve the inherent randomness of the OLSR jitter. Also, it is assumed that cryptographic key distribution between nodes is completed without risk of access by a malicious third party. The study of the effectiveness of the different options available for various levels of cryptographic strength is beyond the scope of this thesis with the assumption that the cryptographic

portion of this thesis is a “pluggable ” aspect of design with the degree of cryptographic security required to meet the application.

The nodes communicating covertly are considered to be friendly and not compromised. Only attacks against the OLSR routing scheme, via wormholes, or eavesdropping are considered. Wormholes are modeled as being passive in the sense they are not actively dropping packets. Systems of re-syncing cryptographically keyed traffic between nodes exist [20][21][22], but are outside of the scope of this thesis. It is assumed that if a HELLO packet is dropped the receiver simply advances the keyed jitter stream by one position².

In order to gauge the effectiveness of the error correction coding schemes utilized within this thesis, it is best to contrast the results to theoretical expected maxima. The limiting factor of timing-delay manipulated covert message traffic between nodes is the sensitivity of the transmitting and receiving nodes signal sampling hardware. Thus, it is assumed that the smallest unit of measurement possible, by receiving hardware as required by the OLSR protocol, is the minimum back-off interval slot time of 20 μ s as specified in IEEE 802.11 [9]. As some of the tools used in this thesis are able to measure units as small as 1 μ s this is also considered exceeding the bounds of the IEEE standard.

² A wormhole is free to manipulate all traffic including HELLO message traffic, but to drop HELLO packets is ineffective as this defeats the effect of the wormhole. The methods considered in this thesis examine HELLO message delays and are independent of HELLO message content.

3 Chapter: The Covert Channel

This chapter introduces the design of the covert channel and examines the factors contributing to channel noise. Theoretical channel capacity using Shannon's theory [23] is formalized as pertaining to a covert channel over OLSR using HELLO message. Receiver detection and error correction coding techniques are also introduced as applicable to this study to mitigate noise and increase throughput.

3.1 Modeling the Channel using HELLO Message Traffic

This section begins with the HELLO message jitter techniques as introduced in [15] and presents a model for channel noise.

3.1.1 Communicating with Message Jitter

The concept of using simple timing channels for covert communication is introduced in [24] and [25]. These methods can be applied to almost any medium, and in this thesis, they are adapted to the jitter portion of the OLSR HELLO message protocol. The functioning premise is that the amount of time a HELLO periodic message is delayed represents a symbol. In the absence of noise and using a discrete sampling function, the capacity of the channel is limited to the information conveyed by each symbol and the maximum possible number of symbols in the alphabet. As the proposed covert channel uses delay over a fixed interval to convey a symbol, it is limited to the maximum number of possible symbols, which is limited to quantization of the transmitter and receiver over the prescribed interval with a mathematical maximum as presented later on in the chapter.

Consider a message that is transmitted periodically, such as every two seconds in the case of OLSR HELLO message traffic as per RFC 3626 [4]. If it is possible to delay the transmission of the periodic message by a specific amount of time it would then be

possible for the receiver to distinguish this delay as a symbol, independent of the actual message sent, which is the basic tenant of the simple timing channel as proposed by [25].

In order to be truly covert the action of delaying transmission of a message must be consistent with the terms of the underlying protocol so as not to arouse “statistical suspicion”. In the case of OLSR the application of covert messages is realizable, as demonstrated in [15], through the express terms of the protocol itself. In order to ensure multiple nodes do not transmit their HELLO messages at the same time a random jitter value is subtracted from the HELLO_INTERVAL of two seconds as per [4], shown in Equation 3. The i^{th} actual HELLO interval is defined by subtracting the i^{th} random jitter value from a fixed HELLO_INTERVAL from.

$$Actual\ HELLO\ interval[i] = HELLO_INTERVAL - jitter[i]$$

Equation 3: OLSR Message Interval

The jitter is limited to a randomly selected value between 0 and $\frac{K}{4}$, as per [4], where K is the HELLO message interval of two seconds.

The approach taken in this thesis is to substitute the randomly selected jitter value with a message value that is obscured by a cryptographically strong pseudo random number generator given some shared secret seed value, for the purpose of conveying a covert message. This allows the sender to manipulate a hidden message with a cryptographically generated key value; this hidden message is sent as the jitter, $jitter[i]$, in Equation 3. At the receiver it is then possible to generate the same cryptographic key stream, using pre-shared keys, and remove this value from the expected HELLO interval to regain the hidden message contained in the remaining deliberate jitter value. This is demonstrated in Figure 4 where the message, conveyed using deliberate jitter, $T_{DJ}[i]$, is

manipulated with a key value, $T_{KJ}[i]$, shared between sender and receiver. At the receiver side $T_{KJ}[i]$ is removed resulting in the original message conveyed with $T_{DJ}[i]$.

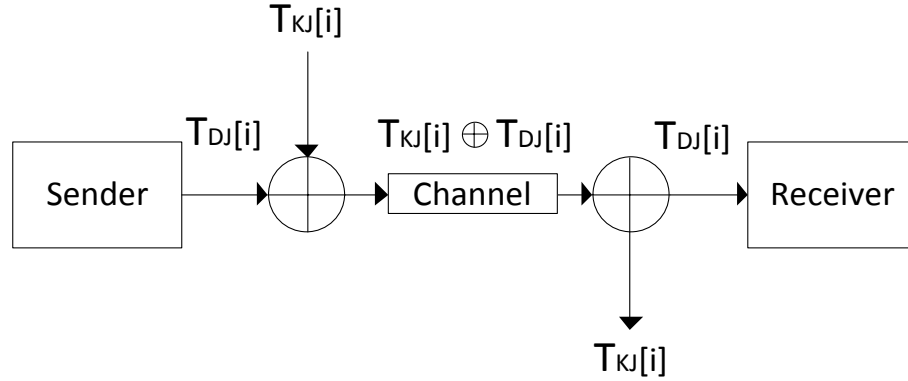


Figure 4: Covert Channel Mechanism

Covertness of the channel is maintained as the purpose of jitter induced delay is already an integral part of the protocol and therefore does not break any expected operating norms. A more thorough discussion of stealth is presented later in Section 4.1.

The conceptual model presented above is lacking with respect to the addition of noise introduced through additional delay factors that need to be considered in real world systems. In any system using a protocol stack, as implemented in this thesis, there will exist delays inherent in protocol stack traversal, such as CPU and operating system overhead to name a few. An analysis of all the specific delays inherent in an OLSR system has already been conducted in [3]. In this thesis all delays are amalgamated into one variable, T_A , representing all unknown random jitter present in the system. Mitigating the effects of the variable T_A , on the proposed covert channel, through the use of error correction coding theory will be the focus of this thesis and central to the results in Chapter 6.

To better understand how T_A affects the covert channel consider the following model in Equation 4 where Δt represents the time between successive HELLO messages as measured by the receiver. T_{HP} is the HELLO_INTERVAL, or two seconds, as per the OLSR protocol. $T_{DJ}[i]$ is the i^{th} deliberate jitter XORed with the i^{th} keyed jitter, $T_{KJ}[i]$, used to encrypt $T_{DJ}[i]$ and ensure jitter values are uniformly distributed. The remaining uncontrolled element is $T_A[i]$ representing the unknown jitter random variable caused by message handling overhead between successive sender delay, denoted as $T_{SD}[i]$, and receiver delay, denoted as $T_{RD}[i]$ as shown in Equation 4. For a detailed breakdown of all the contributing factors associated with these delays the reader is directed to [3].

$$\Delta t = T_{HP} - (T_{KJ}[i] \oplus T_{DJ}[i]) + T_A[i]$$

$$T_A[i] = T_{RD}[i] + T_{SD}[i] - T_{RD}[i - 1] - T_{SD}[i - 1]$$

Equation 4: HELLO Message Covert Channel Calculation

After measuring Δt and removing the known value of T_{HP} the remaining result of $(T_{KJ}[i] \oplus T_{DJ}[i]) + T_A[i]$ is passed to the receiver which estimates $(T_{KJ}[i] \oplus T_{DJ}[i])$ then removes $T_{KJ}[i]$ to recover the original message, $T_{DJ}[i]$. In reference with [3] this is known as HELLO-periodic HELLO message timing.

At this point, it is possible to demonstrate the effects of T_A on the covert channel implementation using HELLO message jitter delay show in Figure 5.

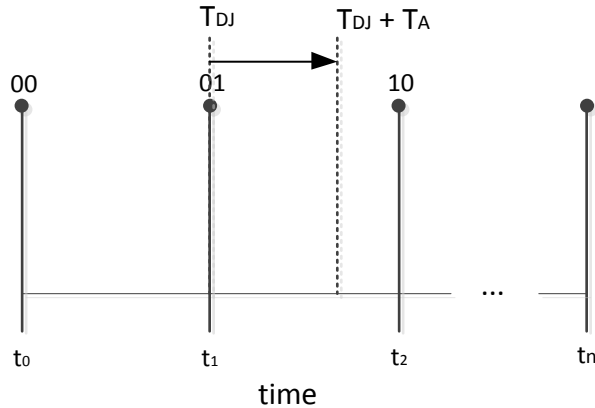


Figure 5: Simple Binning with Delay Added

In this example the intended covert symbol, $T_{DJ} = 01$, is delayed between the sender and receiver by T_A . This causes the received symbol to appear closer to the value 10. The receiver could then incorrectly decode the symbol to be 10 when 01 was the transmitted symbol. Techniques introduced in this thesis are designed to mitigate the errors from delay introduced by T_A .

3.1.2 Receiver Noise and Delay

An alternative way to represent T_A is shown by the sequence diagram in Figure 6 where the elements of Equation 4 are shown with the unknown delays shown by the darker boxes. Should all delays on both the sender and receiver be fixed constants T_A would reduce to zero, but due to the complexities of stack propagation, CPU overhead and other priority schemes within computing hardware these delays will vary. A more detailed discussion of all the potential delays inherent in a system has already been produced in [3] and is therefore only summarized here as pertaining to the determination of T_A . Should a wormhole be present an additional variable is introduced, T_{WD} , representing the additional delay added from the wormhole.

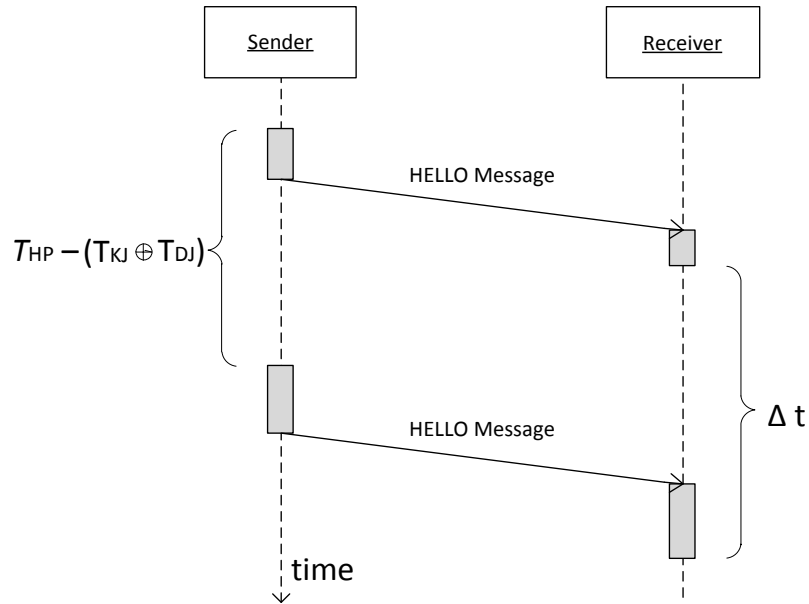


Figure 6: HELLO Message Sequence Chart

The addition of the wormhole results in a sequence diagram as shown in Figure 7 (next page) with the black delay boxes. For the purposes of this thesis the additional delay caused by a wormhole has already been demonstrated in [5] [16] as a random variable with an associated Rayleigh probability distribution ($\sigma=0.002s$). Therefore in the presence of a wormhole the value of $T_A[i]$ is shown in Equation 5. It has been shown previously in [3] that the difference in statistical properties of T_A between samples recorded with and without the presence of a wormhole can be used as a means to detect a wormhole attack. This thesis focuses on this concept.

$$T_A[i] = T_{RD}[i] + T_{WD}[i] + T_{SD}[i] - T_{RD}[i - 1] - T_{WD}[i - 1] - T_{SD}[i - 1]$$

Equation 5: T_A Calculation with the presence of a wormhole

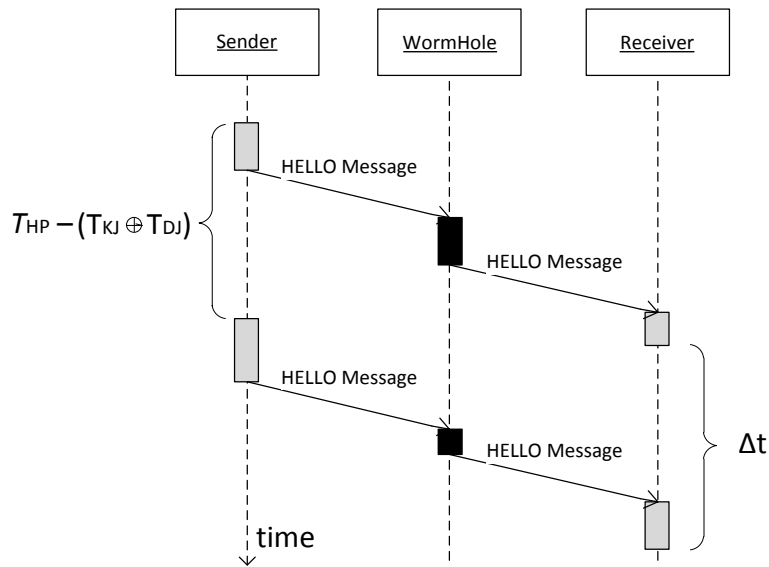


Figure 7: Wormhole Message Sequence Chart

3.2 Calculating Channel Capacity

In order to better understand the practical limitations of a covert channel mechanism over OLSR an understanding of the channel capacity is required. The following sections serve to offer background pertaining to theoretical channel capacity in both the noiseless and noisy channel cases. The theoretical background will be utilized in the results section as a guide to the overall effectiveness of any suggested coding schemes or measures aimed at reducing channel BER.

3.2.1 Capacity of a Noiseless Channel

HELLO message timing intervals are defined within [4] to be limited to a period of two seconds, defined by K , with an accepted jitter limited to a uniform distribution with a maximum range of $[0, K/4]$ per each HELLO message interval. It has been previously proposed that a covert channel can be created by modulating HELLO message traffic between a sending and receiving node [5, 15]. The overall capacity, C , of a

noiseless discrete point to point timing channel is given by [23] and modified by [25] as written in Equation 6.

$$C = \lim_{t \rightarrow \infty} \sup \frac{\log_2 N(t)}{t}$$

Equation 6: Capacity of a Discrete Noiseless Channel

Here $N(t)$ defines the number of unique symbols that can be represented over an interval of time t . As the HELLO message period, t , is limited by K , the HELLO message interval, the model for noiseless capacity can be modified to Equation 7 as discussed in [26] where M is the total number of symbols. Symbols are defined using a specific interval, or bin, limited to the minimum channel quantization T_Q achievable by the receiving node. This is limited by the maximum allowed jitter range of $[0, K/4]$, and symbol count, M with N bits per symbol, shown in Equation 8.

$$C = \frac{\log_2 M}{K}$$

Equation 7: Modified Discrete Noiseless Channel Capacity

$$T_Q = \frac{(K/4)}{M}, M = 2^N | N \in \mathbb{Z}^+$$

Equation 8: Channel Quantization

Equation 7 shows that the receiving node quantization must double for each additional bit in channel capacity C per period K . In practical terms the limiting factor may be the capabilities of the hardware in the noiseless case.

A current hardware limitation for quantization, T_Q , can be approximated by the IEEE 802.11 standard's [9] smallest resolvable time slot, the back-off interval slot time, which is 20 μ s. Using Equation 8 this gives $M = 25000$ possible symbols which

approximates to a 14.6 bit capacity per period, K , or 7.3 bps under noiseless conditions as a current theoretical maximum assuming discrete time intervals and no channel noise.

3.2.2 Deriving the Capacity of a Noisy Channel.

As a noiseless communication channel between nodes represents an unrealistic assumption towards communication, a more accurate upper bound of expected capacity is sought. Guidance is derived from the previous methods proposed by C.E. Shannon's: Theory of Communication [27]. The broad concepts discussed in this section include: Self-Information, Entropy and Mutual Information which are used in Shannon's equations to compute channel capacity for a noisy channel. Here these concepts are applied to find the capacity of the HELLO message timing delay based covert channel.

3.2.3 Self Information

Self information relates to a measure of information about the outcome of events with a defined set of probabilities. Consider a random variable X , which can take on a number of values. When a particular occurrence of $X = x[j]$ is observed this relates to a measurable unit of Self Information of that specific occurrence satisfying three properties:

1. The probability of an event is inversely proportional to the amount of information received from its occurrence.
2. An event that occurs with ultimate certainty gives no information.
3. If the observance of $x[j]$ can be represented by two successive and independent, or mutually exclusive events, then the information rendered is equivalent to the sum of information from observing both events independently.

The above series of properties can all be satisfied by Equation 9 where $P(x[j])$ represents the probability of the occurrence of the event $x[j]$.

$$I(x[j]) = \log_2 \frac{1}{P(x[j])}$$

Equation 9: Self Information

The logarithmic base of Equation 9 is chosen to be two, so as to measure information in units of bits, consistent with the previous section, and is a measure of the information associated with the observance of a particular event.

A sample application of this equation is illustrated by observing the amount of information conveyed by the outcome of the toss of a two sided coin toss where each face of the coin occurs with probability of one-half. This will convey $\log_2(2)$ or one bit of information, either on the observance of a “heads” or “tails” assuming the probability of each event is equal.

3.2.4 Entropy

While Equation 9 gives a defined amount of information from a specific occurrence of the event $x[j]$ the average *self information* of a random variable is called the entropy. The following formula provides a definition of the entropy associated with the random variable X which is consistent with the properties of *self information* and measured in bits.

$$H(X) = \sum_j P(x[j])I(x[j]) = \sum_j P(x[j])\log_2 \frac{1}{P(x[j])}$$

Equation 10: Entropy of a Random Variable

Applying this to the example using a two sided coin gives $H(X) = 1$ bit of entropy for a single coin toss.

3.2.5 Mutual Information

Adding further to the previous section, consider two random variables whereby the output of X is denoted by $x[j] \ / j \in \mathbb{Z}^+$ and the outcome of Y is denoted by $y[k] \ | \ k \in \mathbb{Z}^+$. Consider the case where the event $y[k]$ is observed. In order to establish how much information the observation of $y[k]$ conveys about the occurrence of the event $x[j]$ a definition of mutual information is required. Staying consistent with the properties of *self information* the following properties are required for mutual information:

1. If the random variables X and Y are independent their observance of $y[k]$ provides no information about the occurrence of $x[j]$, therefore there is zero mutual information.
2. If the random variables X and Y are equal then the observance of $y[k]$ provides all required information about the occurrence of $x[j]$ and would equate to the measure of *self information* of $x[j]$ as per Equation 9.

Mutual information is therefore defined in the following equation where $I(x[j], y[k])$ is the mutual information between $y[k]$ and $x[j]$ with $P(y[k] \ | \ x[j])$ as the conditional probability of $y[k]$ given $x[j]$ has occurred and $P(y[k] \cap \ x[j])$ is the probability of $x[j]$ and $y[k]$ occurring jointly.

$$I(y[k], x[j]) = \log_2 \frac{P(y[k] \ | \ x[j])}{P(y[k])} = \log_2 \frac{P(x[j] \cap \ y[k])}{P(x[j])P(y[k])}$$

Equation 11: Mutual Information of Two Events

The average mutual information of two random variables is found in Equation 12 by finding the expectation of Equation 11 over all $x[j]$ and $y[k]$. A logarithmic scale of base 2 is used to obtain the average mutual information in bits.

$$I(X, Y) = \sum_j \sum_k P(x[j] \cap y[k]) I(x[j], y[k]), \text{ or}$$

$$I(X, Y) = \sum_j \sum_k P(x[j] \cap y[k]) \log_2 \frac{P(x[j] \cap y[k])}{P(x[j])P(y[k])}$$

Equation 12: Average Mutual Information of Two Random Variables

3.2.6 Noisy Channel Capacity Calculations

It is now possible to provide a mathematically derived upper bound for the expected capacity of a channel transmitting in the presence of additive noise. Assume a system as demonstrated in Figure 8. Here, X represents the signal input random variable synonymous with T_{DJ} as sent from the transmitter from Section 3.1.1. Y denotes the output random variable altered as a result of the noisy channel and represents the value of $T_{DJ} + T_A$ as observed by the receiver. Both X and Y are discrete random variables with a probability that $y[k]$ is received given $x[j]$ was sent of $P(y[k] | x[j])$.

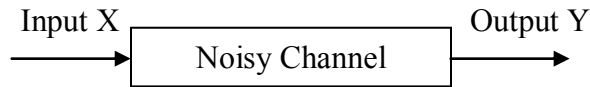


Figure 8: Communication over a Noisy Channel

Channel capacity, C , is measured in bits per channel use, or period in the case of HELLO message traffic over OLSR, and represents the theoretical maximum error free information transfer rate between a transmitting and receiving node. The capacity is defined then by the maximum mutual information resulting between the input X and output Y where $I(X, Y)$ is maximized over the set of all possible input probabilities, $P(x[j])$ as shown in Equation 13.

$$C = \max_{P(x[j])} I(X, Y) = \max_{P(x[j])} \sum_j \sum_k P(x[j])P(y[k] | x[j]) \log_2 \frac{P(y[k] | x[j])}{P(y[k])}$$

Equation 13: Discrete Capacity over a Noisy Channel

Capacity then depends on $P(y[k] | x[j])$. However, as $y[k] = x[j] + T_A$ this implies that $P(y[k] | x[j])$ depends entirely on the noise statistics of T_A . Equation 13 represents the scenario whereby the transmitter's input into the channel and the receiver's output from the channel are limited to discrete values. In the context of the proposed covert channel communication mechanism from Section 3.1.1, the transmitter is limited to a fixed number of possible symbols which translates into a discrete set of potential delays between $[0, K/4]$. $P(y[k])$ is the total probability of Y . Equation 13 is best suited for application where the sender and receiver use fixed bin sizes, limited by T_Q and "hard decisions", of being in either one bin or another, in regards to $y[k]$. This is demonstrated in Figure 9 where $y[k]$ must either be interpreted as $x[j+1]$ or $x[j+2]$ using a hard decision technique.

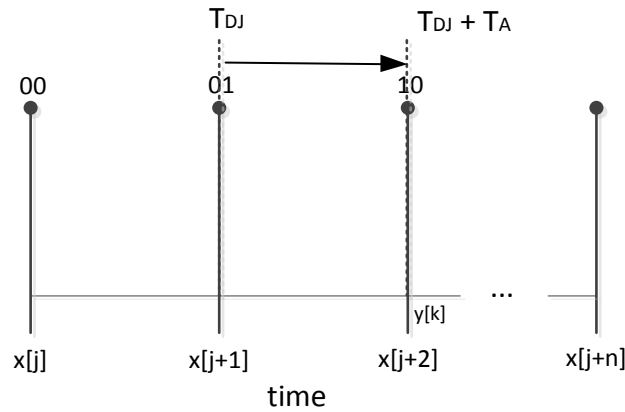


Figure 9: Discrete Binning with Delay Added

For the HELLO message jitter manipulated covert message passing, the input X is limited to a discrete set of values, limited to M slots between 0 and $K/4$. The output value, Y , however may not be limited to a set of discrete points. This is demonstrated in Figure 10 similar to Figure 5 where the generic time values, t , are replaced by the transmitter slot times; $x[j]$. Here the receiver can determine the exact continuous value for received time,

$T_{DJ} + T_A$, and does not need to round to the nearest value of $x[j+2]$ as in the discrete-discrete case from Equation 13.

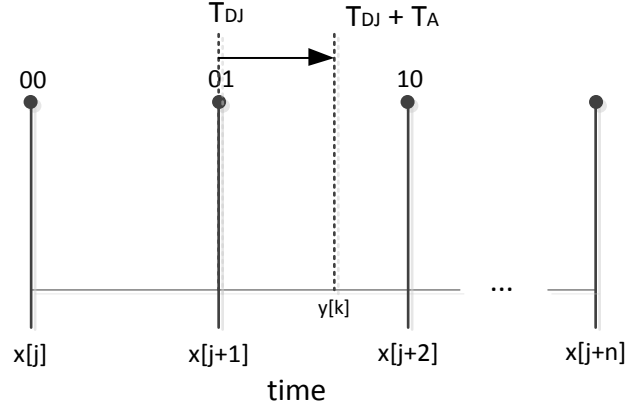


Figure 10: Semi Discrete Binning with Delay Added

Should Y be continuous with a discrete input value X it is shown that Equation 13 changes to the semi-discrete case where Equation 13 is modified to produce Equation 14. Here the receiver can record the exact value associated with the observed value of $y[k]$. Being able to record the added information associated with difference between $y[k]$ and $x[j+1]$, using Figure 10 as an example, allows for the use of “soft decision” methods that can evaluate probabilities with more precision based on a series of measurements. $p(y | x[j])$ becomes the conditional probability density function of Y given $x[j]$ has been sent. $p(y)$ is again the total probability of Y .

$$C = \max_{P(x[j])} I(X, Y) = \max_{P(x[j])} \sum_j \int_{-\infty}^{\infty} P(x[j]) p(y | x[j]) \log_2 \frac{p(y | x[j])}{p(y)} dy$$

Equation 14: Semi-Discrete Capacity over a Noisy Channel

Equation 14 is best suited to determining the upper bounds of the covert channel with inputs $x[j]$ defined by the channel quantization from Equation 8 as messages are sent from the transmitter. At the receiver side it is assumed, in accordance with previous

statements, that the receivers' quantization is limited to the IEEE 802.11 standard's [9] smallest resolvable time slot, the back-off interval slot time, which is $20\mu\text{s}$. Equation 14 is then approximated using a transmitted message, $x[j]$, with a slot size of T_Q from Equation 8 and a received message slot size, $y[k]$ of $20\mu\text{s}$. This translates to using fixed sender bin sizes, limited by T_Q and soft decisions in regards to $y[k]$. The total probability, $p(y)$, is approximated using Equation 15. Additionally, as X is determined to be uniformly distributed, as per the requirements of the OLSR protocol, $P(x[j])$ will become a fixed constant equal to $\frac{1}{2^N}$ where N is the number of bits used to quantize the channel.

$$p(y) = \sum_j p(y | x[j])P(x[j]) \cong \sum_k \sum_j P(y[k] | x[j])P(x[j])$$

Equation 15: Approximation of Total Probability

In order to find the highest possible theoretical capacity of the covert channel in the presence of noise, any limitations of sender and receiver quantization are eliminated. This is expressed in Equation 16 where $p(x)$ is defined by the probability density function (pdf) of the uniform random variable with $f_x(x) = \frac{4}{K}$ with $x \in [0, \frac{K}{4}]$ and $p(y)$ as the total probability of Y as per Equation 15.

$$C = \max_{p(x)} I(X, Y) = \max_{p(x)} \int_{-\infty}^{\infty} \int_{-\infty}^{\infty} p(x)p(y | x) \log_2 \frac{p(y | x)}{p(y)} dy dx$$

Equation 16: Continuous Capacity over a Noisy Channel

Equation 14 and Equation 16 become useful to gauge the effectiveness of the chosen encoding schemes used during simulation and experimental results against the effective channel capacity limitations. They will also offer additional insight into the best

choice of N (bits per symbol) used by the system given the properties of the measured noise in the channel.

In Chapter 6 these capacity equations will be evaluated for channel characterizations obtained through extensive simulation and compared to channel signal to noise ratio (SNR). Channel SNR is calculated, as adapted from [28], in the discrete case, using a ratio of mean signal, which is channel quantization, to the standard deviation of the noise process, T_A , as per Equation 17.

$$SNR (dB) = 20 \log_{10} \frac{T_Q}{std[T_A]}$$

Equation 17: SNR of Discrete Channel

3.3 Receiver Detection Theory

Techniques that may serve to further reduce the bit errors can be applied by the receiver of a covert message and should be examined first before introducing additional overhead associated with error correction coding. This section examines these techniques.

3.3.1 Maximum likelihood Symbol Detection

Given the receiver has an understanding of the noise through the distribution of T_A it becomes possible to make decisions based on the probability of a symbol, $x[j]$, being sent where $x[j]$ denotes a discrete symbol between $[0, M)$. The receiver can estimate the most likely symbol, $x[j]$ transmitted, given a continuous value, y , is observed at the receiver. This is formalized in Equation 18 using Bayes' Rule. That is, the receiver can estimate the value $x[j]$ that maximizes $P(x[j] | y)$ as expressed in Equation 18.

$$P(x[j]|y) = \frac{p(y|x[j])P(x[j])}{p(y)} = \frac{p(y|x[j])}{M \sum_j p(y|x[j])}$$

Equation 18: Maximum likelihood Symbol Detection

The reduction realized on the right hand side of the equation is possible by assuming $P(x[j]) = \frac{1}{M}$ due to the nature of the uniform distribution of symbols. The probability of y , denoted $p(y)$, is the summation of all probabilities of a particular observed value, y , given all possible inputted discrete symbols, $x[j]$.

The selection of $x[j]$ is found by choosing the symbol $x[j]$ that maximizes the value of Equation 18. This is called the maximum likelihood detector. In Section 6.2.1, it is found that a maximum likelihood symbol detector for the covert channel functions as a simple minimum distance detector.

3.3.2 Maximum likelihood Sequence Detection

Should the receiver maintain a memory of all received symbols, as implied through the use of larger codes which are subdivided into particular block sizes for transmission, it is possible to make statistical predictions from the received sequence vector, $\mathbf{y} = (y_1, y_2, \dots, y_n)$ observed by the receiver for a given vector of transmitted symbols $\mathbf{x} = (x_1[j_1], x_2[j_2], \dots, x_n[j_n])$. In this case Equation 18 can be represented using Equation 19.

$$p(\mathbf{x}|\mathbf{y}) = \frac{p(\mathbf{y}|\mathbf{x})}{p(\mathbf{y})} = \frac{\prod_{i=1}^n p(y_i|x_i[j_i])}{\sum_j p(\mathbf{y}|\mathbf{x}_j)P(\mathbf{x}_j)}$$

Equation 19: Maximum Likelihood Sequence Detection

In maximum likelihood sequence detection, then, the receiver chooses the sequence \mathbf{x} that maximizes $\prod_{i=1}^n p(y_i|x_i[j_i])$.

3.3.3 Gray Mapping

Gray Mapping, originally patented by Frank Gray at Bell Telephone [29], is a method of mapping bits to symbols so as to ensure the bitwise difference between two adjacent symbols, or Hamming distance, is one bit. For example, the binary sequence 00, 01, 10, 11 becomes 00, 01, 11, 10 after Gray Mapping. The advantage of this scheme is that when errors or noise are introduced into a system such that adjacent symbols may be mistakenly received the resulting bit error is minimized. To best illustrate this observe the symbol mapping in Figure 11. This depicts $M = 2^7$, or 7-bit symbols. The advantage can be seen when in the standard binary coding scheme the binary value 00001111 is transferred and additional noise, sufficient enough to cause displacement by a half-symbol, will cause a 4-bit error from the decoded value of 00010000 with a Hamming distance of four. When Gray Mapping is applied the Hamming distance is reduced to one bit for adjacent symbols.

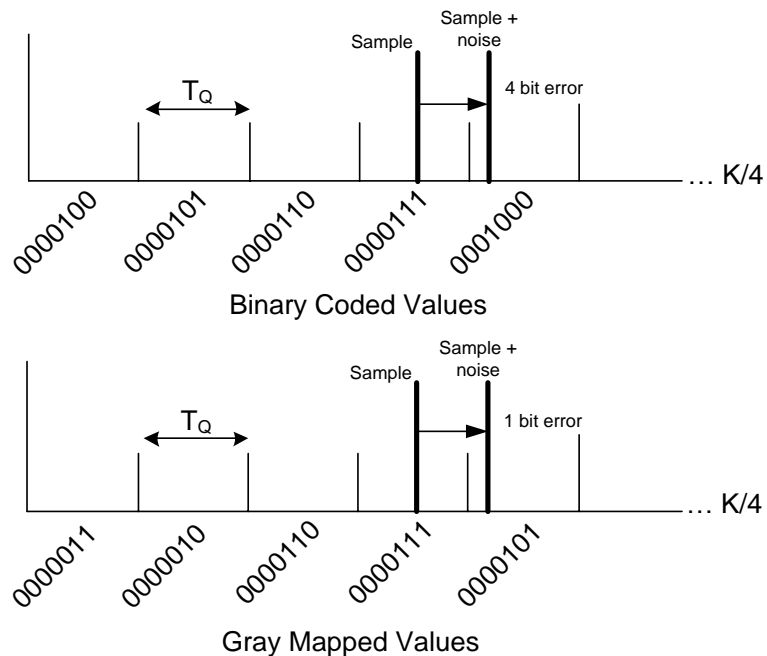


Figure 11: Gray Mapping Example

3.3.4 Symbol Reliability with Bit Log-Likelihoods

The output from a Maximum Likelihood Symbol Detector, as discussed in Section 3.3.1, is a decision on the most probable symbol received. It is sometimes desirable, however, for the receiver to further compute the likelihood of receiving each individual bit in every symbol, as opposed to simply computing the most likely symbol. This is of particular importance when using a Viterbi decoder for soft decision decoding, discussed in Section 3.4.3, whereby a specific confidence rating is assigned to each bit input to the decoder.

The concept of bit-reliability is demonstrated in Figure 12. In this example Symbol sizes of $N = 2$ are chosen and ordered using Gray Mapping, from Section 3.3.3, at widths of T_Q from Equation 8. The received delay, y , is shown between two symbols, $x[2]$ and $x[3]$, respectively. In a “hard decision” decoding scheme y would be interpreted as its closest neighboring symbol, as $x[2] = 11$ in this case. When examining the reliability of the individual bits associated with the received symbol it is possible to predict the received symbol to a higher degree of precision. Of the two adjacent symbols to y , being $x[2]$ and $x[3]$, when examining the left most significant bit (MSB) and least significant bit (LSB) different probabilities arise.

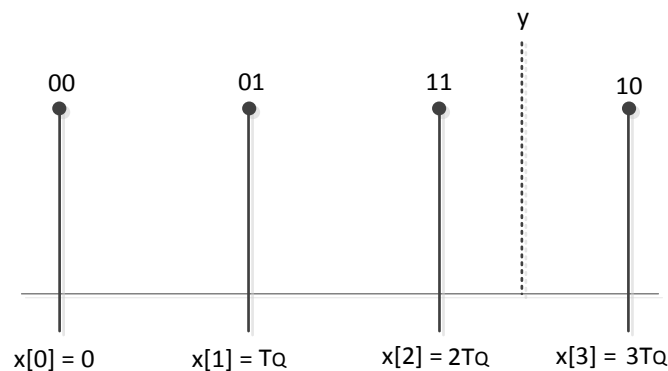


Figure 12: Bit Log-Likelihood Example

It can be seen that of the adjacent potential symbols the likelihood of the MSB being interpreted as the value “1” is greater than the LSB being interpreted as the value “1” for a message received at delay, y . In this scheme the likelihood of the LSB being decoded in error is greater than the likelihood of the MSB being decoded in error. The only chance of the MSB being incorrectly interpreted is by a larger error delay from the transmitted delay.

In order to mathematically quantify this relationship the following notations is adopted. The bit-wise representation of any symbol becomes $B_1B_2..B_n | B_j \in (0,1)$ where B_j represents each individual bit position in the symbol from MSB to LSB. Given an observed delay, y , the probability of $B_j = “1”$ or “0” is defined by the likelihood, $p(y | B_j=1)$ and $p(y | B_j=0)$. Therefore the Log-Likelihood Ratio (LLR) is described using Equation 20.

$$LLR_j(y_i) = \log \frac{p(y_i | B_j = 1)}{p(y_i | B_j = 0)}$$

Equation 20: Log-Likelihood Ratio for bit, B_j

The value derived from $LLR_j(y_i)$ represents the reliability of bit B_j . A negative value indicates a greater reliability towards $B_j = 0$, while a positive value gives a higher reliability towards $B_j = 1$. In order to evaluate Equation 20 the numerator and denominator must consider all the symbols whereby $B_j = 1$ and $B_j = 0$. Using the notation $x_1[j] | j \in (0, \dots, 2^N)$ to denote all the symbols where $B_j = 1$ and $x_0[k] | k \in (0, \dots, 2^N)$ to denote all the symbols where $B_j = 0$, Equation 20 becomes Equation 21.

$$LLR_j(y_i) = \log \frac{\sum_{x[j] | B_j=1} p(y_i | x_1[j])}{\sum_{x[k] | B_j=0} p(y_i | x_0[k])}$$

Equation 21: Log-Likelihood Ratio for bit, B_j of the Covert Channel

Applying Equation 21 to the example shown in Figure 12 yields the Equation 22 and Equation 23 as shown below.

$$LLR_1(y) = \log \frac{p(y_i|x[2]) + p(y_i|x[3])}{p(y_i|x[0]) + p(y_i|x[1])}$$

Equation 22: Bit Log-Likelihood Example B_1

$$LLR_2(y) = \log \frac{p(y_i|x[1]) + p(y_i|x[2])}{p(y_i|x[0]) + p(y_i|x[3])}$$

Equation 23: Bit Log-Likelihood Example B_2

The values associated with LLR_1 and LLR_2 can be used as soft inputs into a Viterbi decoder as examined in the results, Section 6.3.2. This is done in order to establish finer detail concerning the mostly likely bit sequence, as opposed to symbol sequence, received given the modeled channel noise, from Section 3.1.2.

3.4 Improving the Model with Coding Theory

The following section discusses the relevant background concerning the improvements to the basic premise of binning message symbols as introduced in [3] [5] by using error correction coding theory. The approach is aimed to reduce BER and improve throughput under noisy conditions as well as provide indicators for the detection of a wormhole.

Error correction coding offers a method of introducing redundancy into a transmitted message which allows the receiver to recover the original message despite the addition of noise. The binary coding schemes examined here add redundancy to binary message traffic in a mathematically predictable fashion, which serves as the basis for error correction within the proposed covert channel. However, there is a cost in that given a fixed rate of traffic in a channel the code portion of a coded message will consume throughput normally used by actual message traffic. For example a code requiring $n = 7$

bits of coded message with $k = 4$ actual message bits actually sent. From inspection $n - k$, or 3 bits, are consumed by the encoding scheme for a total message information size of k bits.

3.4.1 Block Coding Schemes

In the linear block coding schemes a k -bit message block is mapped to an n -bit code block such that $n > k$. The code rate R , is expressed as $R = \frac{k}{n}$, which indicates the ratio of k message bits to n code bits. The block code notation is written as (n, k) where n represents the length of the code words and k represents the length of the message words. Block coding schemes can be described as using a vector $\mathbf{D}_i = [d_{i1}, d_{i2}, \dots, d_{ik}]$ representing the i^{th} k -bit message word where d represents each bit in the message. The associated code word vector becomes $\mathbf{C}_i = [c_{i1}, c_{i2}, \dots, c_{in}]$. As \mathbf{D}_i is limited to 2^k possible messages, and since $n > k$ there is a level of redundancy inherent in this scheme. The relationship between \mathbf{D}_i and \mathbf{C}_i is characterized through the $k \times n$ generator matrix, \mathbf{G} , as seen in Equation 24.

$$\mathbf{C}_i = \mathbf{D}_i \mathbf{G}$$

$$\mathbf{G} = \begin{bmatrix} g_{11} & g_{12} & \cdots & g_{1n} \\ g_{21} & g_{22} & \cdots & g_{2n} \\ \vdots & \vdots & \ddots & \vdots \\ g_{k1} & g_{k2} & \cdots & g_{kn} \end{bmatrix}$$

Equation 24: Block Coding Generator Matrix

Assuming a message, \mathbf{X} , is sent over a channel with noise, \mathbf{N} . The receiver observes message, $\mathbf{Y} = \mathbf{X} + \mathbf{N}$. The value of \mathbf{X} is recovered by finding the code word, \mathbf{C}_i closest to \mathbf{Y} in terms of Hamming distance. Please refer to [30] as recommended textual reference for further background.

Error correctional coding can be used to either correct or detect errors in transmitted message traffic. The error correcting or detection capabilities of a code are determined by the minimum distance, d_{min} , which represents the minimum Hamming distance between two code words. For a code that corrects or detects t errors the required d_{min} is given by Equation 25. As a reference example a Hamming(7,4) code has $d_{min} = 3$ and would be able to correct one bit error and detect up to two bit errors

$$d_{min \text{ correction code length}} = 2t + 1$$

$$d_{min \text{ detection code length}} = t + 1$$

Equation 25: Minimum Hamming Code Distances

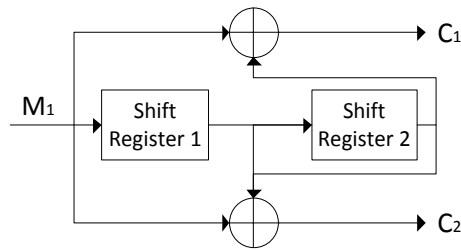
Cyclic block coding is a subset of linear block coding with additional structure added to the codes by imposing that shifts of code words also form new code words. Using the above nomenclature, if $\mathbf{C}_i = [c_{i1}, c_{i2}, \dots, c_{in}]$ is a code word then so is $[c_{i2}, \dots, c_{in}, c_{i1}]$ as an example. This fundamental addition can reduce the required overhead needed during decoding as seen with the BCH family of codes named after their inventors, Raj Chandra Bose, D.K. Ray-Chaudhuri and Alexis Hocquenghem, whose last names comprise the name of the code. BCH codes are among a set of codes that also have the advantage of syndrome decoding, which uses a lookup table to simplify the decoding process and required hardware.

3.4.2 Convolutional Coding

Convolutional codes, introduced in [31], operate in an entirely different nature from block codes and can offer increased error correcting performance at comparable levels of complexity to block coding schemes are key fundamental difference is the decoding process. The decoding process is able to examine a sequence of received symbols and determine the best probabilistic fit, either using soft or hard decisions with

respect to each symbol received whereas block codes usually use only hard decisions. For the purposes of this thesis, both hard and soft decision techniques are examined, as discussed from Section 3.2.6.

To better understand the operation of convolutional codes an example is given. A basic model of a convolutional coding scheme, adapted from [30], is modeled in Figure 13 representing a rate $R = \frac{1}{2}$ code where for every message bit the encoder produces two code bits.



$$G(x) = [1 + x^2 \quad 1 + x + x^2]$$

Figure 13: Simple Convolutional Encoder and associated Transfer Function

The message for the purposes of this example is *11010* (sent from left to right into the encoder). As the initial state of both shift registers, S_1 and S_2 are 0 with $M = 1$, the first outputs equate to $C_1 = M_1 \oplus S_2$ and $C_2 = M_1 \oplus S_1 \oplus S_2$ which resolves to $C_2C_1 = 11$ for $M_1 = 1$. After the generation of the first code bits S_1 updates its state to $M_1 = 1$ with S_2 unchanged at zero. The second iteration with $M_1 = 1$ gives $C_2C_1 = 01$. The value in S_2 and S_1 then become 1 and $M_1 = 0$ which gives $C_2C_1 = 01$. Repeating this procedure renders the coded bits *11 01 01 00 10 11 00* with a code rate, $R = \frac{k}{n} = \frac{1}{2}$. Note that the last four bits are generated from passing an additional two zeros through the code in order to pass through the remaining values in the shift registers.

Convolutional codes are frequently represented using a transfer function, $G(x)$ denoted in Figure 13 using a $k \times n$ matrix ($k = 1$ and $n = 2$ in Figure 13); The zeroth order of the polynomial represents the input at M_1 ; the first order is S_1 and second order S_2 . Therefore the left element in $G(x)$ indicates that its output is the exclusive-or of the input, M , and the second shift register, S_2 . It is also possible to abbreviate the polynomial using octal values, therefore the generator matrix can also be expressed as $G(x) = [5 \ 7]$. The coded bit C_1 is generated in the first column and C_2 in the second.

At the decoder side a Trellis Diagram is constructed, as shown in Figure 14 for illustrative purposes only. The black nodes indicate the possible states of the convolutional shift registers (S_2S_1), with the purpose of the Trellis diagram to represent all the possible state and transitions between states. The format of the state transition mapping is M_1/C_2C_1 which equates to the given state transition given the current state of the shift registers and the message input, M_1 , resulting in the coded bit outputs C_2C_1 .

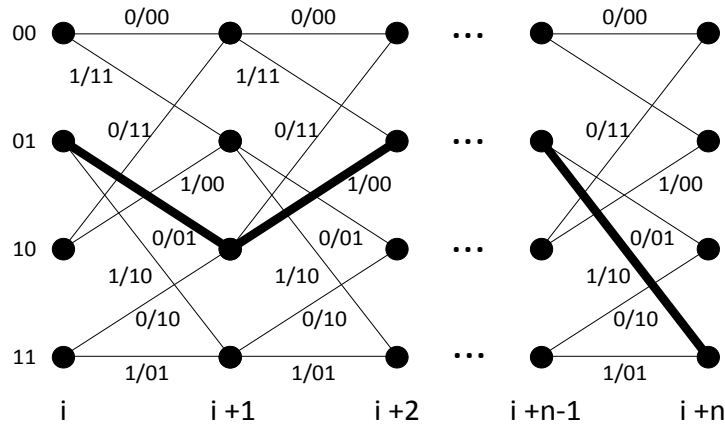


Figure 14: Sample Trellis Diagram

The dark line traced through this sample trellis state is a possible valid path through the trellis. Errors in the received bits may produce an invalid path through the trellis. The Viterbi decoder [32] offers an efficient means to identify the most valid path (i.e path

closest to the received bit sequence), given the errors present. Two options of decision making are possible. Firstly, hard-decisions use the minimum Hamming distance between paths (i.e between received sequence and valid path) to determine the most likely result. The second, and more effective method at the expense of increased complexity, is soft-decision decoding which uses a Euclidean metric.

An important property when examining convolutional codes is the metric, d_{free} , or “minimum free distance” which represents the minimum Hamming distance between any possible paths through the trellis. A general relationship exists between larger codes that have larger free distance properties at the expense of increased complexity. Additionally, convolutional coding lends itself to “bursty” errors, in that when the code fails to correct errors, it fails at a greater scale compared to block coding.

In contrast to block coding schemes, effective convolutional codes are found through exhaustive trial and error searching as pertaining to the application at hand. Pre-determined convolutional codes are used in this thesis using hard and soft decision decoding.

3.5 Complete Covert Channel Systems Perspective.

This section will summarize, from previous sections, the mechanics behind the proposed system of passing covert messages over the channel along with identifiable metrics used in the results in section 6.2 and 6.3 to evaluate the effectiveness of the techniques introduced in the chapter. The following Figure 15 offers a holistic systems view of the proposed covert channel implementation over OLSR.

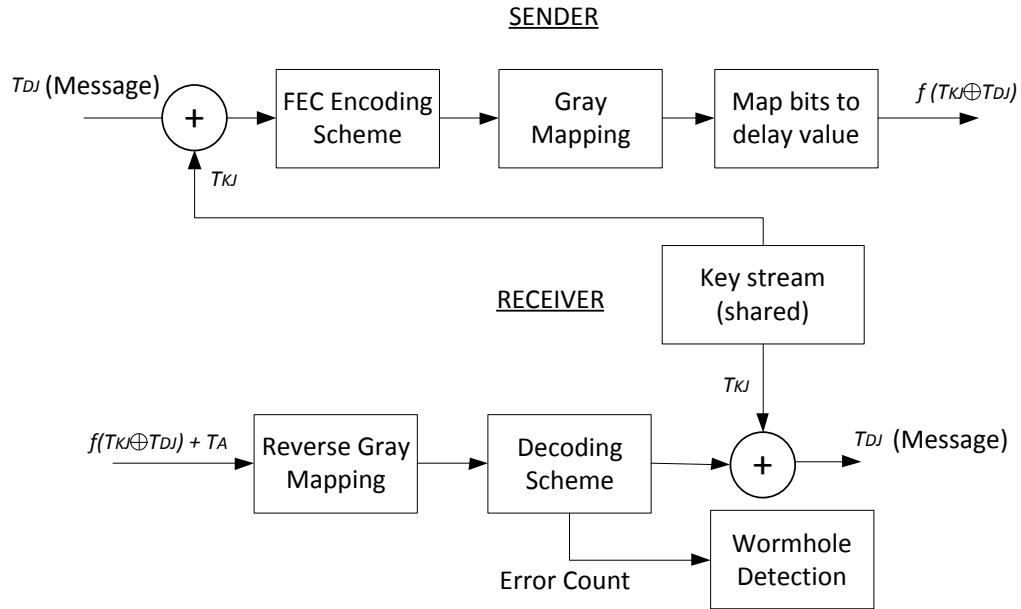


Figure 15: OLSR Covert Channel System

The original message, T_{DJ} , is transformed into $(T_{KJ} \oplus T_{DJ})$ using a cryptographic function that generates the keyed jitter value T_{KJ} , thus the original bit stream is XORed with a cryptographically generated pseudorandom bit stream. Next the transformed bit stream is encoded using an error correction code. As per coding theory, k bits of covert message bits are encoded into n bits of coded message. This thesis will examine a Forward Error Correction (FEC) Scheme chosen from the types discussed previously. The coded message must be divided into N -bit length symbols, limited by the available quantization provided by the maximum number of possible symbols, 2^N . Gray Mapping is then applied to the resulting symbol value between $[0, M)$ to limit the effects of adjacent symbol impacts on BER. The resulting Gray Mapped value is then transformed into a delay jitter value between $[0, K/4)$ resulting in $f(T_{KJ} \oplus T_{DJ})$ to ensure that the overall uniformity of jitter values as visible to a third party remains uniformly distributed.

At the receiver the difference of two successively received HELLO messages is measured resulting in $f(T_{KJ} \oplus T_{DJ}) + T_A$ with noise introduced from additive noise from T_A . Nearest neighbor detection of the symbols is performed in the hard decision case. The N -bit symbols are Gray Mapped back to their binary equivalent value and recombined into the original n -bit code word for decoding by the selected scheme resulting in the value $(T_{KJ} \oplus T_{DJ})$. The receiver can then remove T_{KJ} thus recovering the original sent message, T_{DJ} .

Finally, the receiver can examine the number of corrected errors from the decoder and compare this against an expected norm as a potential indicator towards the presence of a wormhole. The advantage of using error correction, aside from improved channel reliability, is that the receiver corrected errors provide information relevant to the detection of a possible wormhole attack, discussed in the next chapter.

The inherent question becomes how to optimize the code and the selected code rate, R , such as to minimize code overhead and maximize throughput towards the theoretical capacity boundaries while minimizing the BER of the channel. The design elements under control are: (1) selection of the coding and decoding scheme; (2) selection of the maximum allowed number of symbols, M ; and (3) the selection of detector used for determining symbols by the receiver. The selection of key stream is also a controllable aspect, but bears no impact on the optimization of the communications channel in terms of capacity and BER. The design criterion becomes to select the most effective code, R , given a T_A distribution.

4 Chapter: Covert Channel Evaluation

This chapter discusses methods for evaluating channel stealth against potential covert channel detection using statistical analysis techniques as a means to determine how “covert” the channel truly is. Alternative covert channel methods are also discussed in comparison with the covert channel proposed in this thesis from Chapter 3.

4.1 Measuring Channel Stealth

As the proposed jitter channel uses packet delay as a mechanism of communication, the techniques proposed in [33] present a suite of tests aimed at covert channel detection. The Kolmogorov-Smirnov (K-S) test is used to determine the likelihood of one distribution matching another reference distribution to a specified confidence interval. It is possible to see how distribution matching can be used to detect a covert channel if the covert channel alters channel packet delay away from a statistical norm. It functions by examining the largest distances between elements of two probability distributions as a method to predict whether the two sets are statistically similar or dissimilar. Should the largest distance be within the required confidence interval (normally 95%) the null hypothesis, of being equal distributions, is maintained. This is mathematical described in Equation 26. In order for the null hypothesis to be maintained the supremum of the set of distances between the cumulative distribution functions, $F_1(x)$ and $F_2(x)$, needs to be close to zero with appropriate confidence.

$$KS_{Test} = \sup_x |F_1(x) - F_2(x)|$$

Equation 26: Kolmogorov-Smirnov Test Notation

In order to ensure the covert channel, proposed in 3.1.1, is resistant to distribution matching techniques it is important that it be demonstrated that the manipulated jitter

maintains a perfectly uniform distribution comparable to traffic generated without manipulation (i.e un-manipulated OLSR HELLO message traffic).

The K-S method is based on detecting the presence of a covert channel through the detection of statistical difference from a reference distribution, which brings a point of discussion. Should a low channel bit rate be selected, the jitter resolution could become largely discrete. It could become obvious from an observer's perspective that there appear to be finite selected discrete random jitter values inherent in the received samples, which would be a indication of a covert channel, even though uniformly random.

A potential solution proposed here is to start with as close to continuous jitter as possible, a valid assumption is a jitter resolution smaller than the minimum back-off slot size of $20\mu\text{s}$ is acceptable as receiving hardware is limited to discrete samples. The actual discrete message is added to the jitter value, which is known to the receiver. An example is the value $M = [0, 2^{N-1}] \mid M, N \in \mathbb{Z}^+$. This in addition with a continuous real-valued jitter value $J = [0, 1) \mid J \in \mathbb{R}$ (known to the receiver), results in a real number. As long as all jitter outcomes are equally likely the resulting distribution will present more continuous looking outputs.

In order to accomplish a continuous-like jitter value the system must use modulo $K/4$ operations as opposed to the previously proposed exclusive-or case. However, an obstacle to utilizing modulo keyed jitter proposed in this thesis stems from the boundary cases where T_{DJ} is near 0 or $K/4$ such that the addition or subtraction of T_A causes the received symbol to be incorrectly interpreted. For example, should T_{DJ} represent a symbol mapped to $K/4$ and if $T_A > 0$ this symbol will not be interpreted as $K/4$, but most

likely 0 instead as a result of modulo $K/4$ addition (i.e symbol wrap-around). This will introduce a large bit error into the system. A potential solution could provide a guard region between boundary symbols at 0 and $K/4$ sufficient to negate the effects of T_A . Of note, in the presence of a Wormhole these guards would be exceeded which would increase the error rate, due to symbol wrap-around as described earlier which could help in the detection process.

For the purposes of determining T_A , as used in the results Section, modulo $K/4$ keyed jitter is not used. The results are predicated on using exclusive-or operations as a method to preserve confidentiality as previously discussed. The effects of this approach are further examined in Section 6.4

4.2 Covert Channel Side Effects

The unintended side effect of making the covert channel appear random is that it may actually be more “random” than a normal OLSR HELLO message distribution. Although there is no standard implementation of random number generators for wireless devices using OLSR it could be conservatively assumed they will be cryptographically weak in terms of period before the sequence repeats to save on hardware costs. As a bystander may be able to record all successive HELLO message arrival times it is therefore possible to extract a value associated with $(T_{KJ} \oplus T_{DJ}) + T_A$ from Equation 4. It is not possible, from a bystander’s perspective, to solve for T_{DJ} without knowing the jitter keyed element T_{KJ} , but an observance of successive values of $(T_{KJ} \oplus T_{DJ}) + T_A$ may have a longer period than that of a simple random generator. A simple random generator may be employed by standard OLSR implementations and through comparison

of this period with that of a cryptographically keyed model an inference towards the use of strong random jitter is possible as a potential covert channel signature.

The previously mentioned concern is however minimized as “weak” is defined as a random sequence of length of $\sim 2^{31}$ in [35]. With this sequence it would take over a hundred years to complete a period in terms of HELLO message traffic causing minimal operational concern. Additionally, as per [36], cryptographically strong pseudo-random number generators are emerging for constrained hardware, such as mobile sensor nets, facilitating incorporation into their embedded protocol stack software.

4.3 Detecting Wormholes through Statistical Methods

It should be noted that the same principles discussed in the previous section which are used to maintain channel secrecy can become useful tools when examining the channel for the effects of wormhole on the distribution of T_A . The K-S test and the test for regularity are simple tests to implement as predictors of a covert channel. A similar test using variance of T_A has already been proposed in [3] to detect wormholes.

This thesis proposes observing the error rate, as mentioned previously. It is theorized the wormhole will become apparent when a receiver uses error correction to count the number of error it corrects. The receiver will gain greater confidence over time as more samples are collected and error rate is determined. Should the BER be known for a specific measured SNR, it is possible to count the number of errors, using an chosen threshold value, bringing about a decision to enter a “SUSPECT” state.

Even more robustly, if the original symbol sequence is reconstructed against the received symbol sequence it possible to reconstruct the noise distribution as an indicator of wormhole presence.

Alternatively the wormhole could attempt to only operate on non HELLO message related traffic, but in the case of the OLSR protocol HELLO message traffic is used to generate routing information making it the key operative for wormhole manipulation. The wormhole could then only sniff and subvert traffic between adjacent neighbors thus greatly reducing its effectiveness.

4.4 Wormhole Detection Avoidance Techniques

This thesis aims to detect wormholes by observing error rate in the covert channel. However, wormholes may attempt to avoid detection by modifying their behavior. Two potential avenues for wormholes to hide their presence are possible as discussed in [5] and applicable here. As a brief background, [5] used methods of measuring the Power Spectral Density (PSD) from a time series constructed of received HELLO packets as a means of detecting the presence of a wormhole different from the coding techniques used in this thesis, but the discussion of wormhole defensive practices is still relevant.

A wormhole could try to mask its presence by adding an inverse statistical offset to sequential HELLO message traffic. As discussed in [5] assuming the wormhole knows its own delay distribution when re-transmitting a message it could attempt to delay a message for a fixed period of time minus the inverse random delay distribution. This would result in a zero mean distribution making the long term difference in measured delay zero, but wormhole related random delay would still be present between successively received HELLO messages as demonstrated later on and the variance would effectively double as a byproduct of subtracting two random variables.

A more elusive technique is to ensure a fixed delay variable in repeating messages passed through the wormhole. This is equivalent to ensuring that $T_{WD}[i+1]$ is equal to $T_{WD}[i]$, from Equation 5, thus reducing T_A to that shown in Equation 4 in the case of a wormhole, which provides an effective measured difference of zero when comparing successive message delays providing difficulty for the methods discussed in [5]. The introduction of keyed jitter presents a solution as the receiving node can determine an expected distribution of the sender delay, T_{SD} for HELLO messages, given $T_{DJ} = 0$ and only keyed jitter is used. Additional delay, as introduced by a wormhole adds additional noise to this distribution offering possible suspect information. This method incurs the overhead of clock synchronization between sender and receiver, requires that the receiver can determine its own delay distributions, and assumes a negligible propagation delay.

Overall, wormhole delays, in the forms presented here lend themselves to detection making wormhole detection avoidance difficult from the standpoint of an attacker.

4.5 Review of Alternate Covert Channel Methods

This section discusses alternative mechanisms for covert channels in ad hoc networking environments from the routing protocol to the MAC layer. It is noted that many forms of covert communications exists in many other different networking environments, but are considered out-of-scope for this thesis.

A scheme using Ad hoc On-Demand Distance Vector (AODV) in place of OLSR has been proposed in [7]. This scheme recommends the use of the destination identity in route request message traffic as a possible covert channel for up to $\log_2(N-1)$ bits of information, where N is the number of nodes in the network. This mechanism, however,

produces some potential signature data through the observation of AODV route requests with no resulting information being transmitted on the requested route or uncharacteristic abnormalities observed through sequential node route requests. In larger networks, it is expected this would become more difficult to detect, but may still be subject to statistical analysis. The proposed manipulation of uniformly distributed random jitter of HELLO message traffic with cryptographically strong pseudo random number generation is expected to generate uniformly distributed HELLO message jitter independent of messages sent making statistical analysis extremely difficult.

An alternate suggested approach in [7] is described by manipulating the contention backoff procedure using a splitting algorithm approach. This method is predicated on having fierce channel contention and requires a revision of the underlying MAC backoff algorithm. Nodes must also maintain synchronization through the monitoring of channel traffic in order to reconstruct the pathways using in the splitting algorithm for covert communication. An inherent concern with this method exists around the impacts of noise and delay and how this is interpreted by a prospective receiver of covert traffic. The results as discussed in [7] will be used as a basis for comparison.

Methods of implementing a covert channel using 802.11 header information have been proposed in [37] and for other unused header fields at multiple potential layers in [38]. With these types of approaches it may be possible to achieve a larger potential channel capacity, but any deviation from either expected traffic or protocol norms, as required by these approaches, lends to statistical or steganographic analysis.

A similar solution, like the one proposed in this thesis, using packet timing delay is proposed in [39]. In this method a series of packets has its delays reordered to assign a

specific frequency count of delays to a specific covert value of one or zero, compared to a specific symbol associated with a specific delay as proposed in this thesis. The method validates itself as being robust to entropy detection based methods, but operates with BER very sensitive to the standard deviation of noise in the channel with a demonstrated BER of 30% which makes the channel virtually unusable. Applying this approach to HELLO message traffic would also only provide a channel capacity of 1 bit every $K/4$ period assuming only one delay is used to predict that either a one or zero is transmitted. By using more than one delay as a means to further obfuscate any statistical analysis, the capacity is reduced from 1 bit. Although this method proves to be adaptable to a greater number of protocols, the proposed method of OLSR jitter manipulation in this thesis offers higher channel capacity for comparison in the results section.

5 Chapter: Simulation and Experimental Implementation

This chapter discusses the approach and methodology behind the experiments conducted to examine covert channel communications over the OLSR routing protocol. The basic analysis is conducted in an isolated simulation environment to prove the mathematical concept, after which point additional tools are used as a means to present a more realistic understanding of how such an approach would fare in a real-world environment. Each of the following sections discusses various software and hardware tools used in simulation, emulation and in generating a test-bed. The noted difference between emulation and a test-bed is that the emulation involves a software tool that works in real-time and is designed to be compatible with actual hardware, whereas the test-bed uses only real hardware.

This thesis uses ns2 as the primary simulation environment to capture a set of ordered T_A measurements in a MANET with and without a wormhole present. These samples are extracted into MATLAB in order to apply the derived equations for capacity and compare different receiver detection and error correction techniques. As a further means of comparison (i.e emulation and test-bed) Exata Cyber and OLSRd are used generate further T_A samples as explained in the following sections.

5.1 NS2

Network simulator 2 (ns2) originated in 1989, as a software tool for modeling flow and congestion schemes in packet-switched networks. Ns2 is a discrete-event simulator targeted at networking research and over time has become a multi-research collaborative effort, with DARPA support, and is therefore an excellent starting point from which to demonstrate a functional covert message traffic model. Multiple studies

have been conducted evaluating OLSR using ns2 [40][41][42]. Ns2 provides an accurate model of the 802.11 Medium Access Control and Data Link Layers as noted in [43][44]. Further studies, such as [45][46][47], have compared ns2 to test bed scenarios and emulators with a general outcome that ns2 fares well at low node count (<10 nodes) scenarios. As discussed in [45], it is noted that there is a relatively small (~1ms) difference in latency between ns2 and the test-bed scenario, operating with one hop. This is beneficial to this study as all HELLO message traffic is examined on a one hop basis. The research in [45] does however criticize ns2's characterization of network stack propagation delay and some of the delay variables previously discussed at length in [3]. The effects of MAC delay latency variation deviate from expected norms as hop counts increase [45]. Contrary to [45] when examining capacity or packet delivery ratios, ns2 is evaluated to predict very similar results against the *Castadiva* test-bed [47], but less so against the Mobile Network Emulator (MNE) and *GloMoSim* network simulator [46]. Based on its general acceptance ns2 is used in this thesis as a means to predict the effects of channel encoding on improving covert capacity and predicting the presence of wormholes.

UM-OLSR version 0.8.8, developed by Francisco J. Ros in conjunction with the University of Murcia, is utilized as an extension to ns2 in place of the default ns2 OLSR variant. This decision is taken in order to maintain compatibility with previous work by [3] and [5]. Additionally UM-OLSR allows for ease of configuration towards modulating keyed jitter values though extending its object orientated code base.

As ns2 serves as the simulation engine it requires an Object Orientated Tool Command Language (OTCL) script to configure the environment. Initially ns2 is

configured with two nodes separated by 20 meters and configured to send traffic over UDP at Constant Bit Rate (CBR) 2Mb/s in 1500 byte frames with RTS/CTS enabled consistent with 802.11b wireless usage as a reference point. This is chosen in order to provide processing overhead within the simulation to provoke noise in the expected jitter measured at the receiver. From the OTCL script it is possible to inject message traffic as a string of hexadecimal characters. Note that if no symbol is transmitted the key stream would still advance and maintain distribution uniformity. From a cryptological analysis standpoint this provides the additional security as previously discussed by making it more difficult to decipher message traffic. Actual message traffic can start and stop independent of deliberate jitter transmission. In short, a node could simply be transmitting a HELLO message, or it could be transmitting a HELLO message manipulated with a covert symbol without the knowledge of a third party. This is in contrast to the use of encryption on a normal channel where it is at least possible to observe that encrypted message traffic is taking place.

In order to preserve the expected uniform distribution the Crypto++ library is used with the X917RNG³ random number generator with a SHA256 hashed key and AES cipher. The resulting pseudo-random number stream is manipulated with the associated jitter time value of the message according to a specified N bit mapping. As a validation of the effectiveness of this scheme a uniform distribution of jitter values is expected even if the same message is sent repeatedly. At the receiver a minimum distance algorithm is used to bin the received deliberate jitter value and remove the pseudo-random keyed jitter. Note this mechanism requires that the receiver and transmitter cryptographic key

³ X917RNG is a cryptographically secure pseudo random number generator provided with the Crypto++ code library based on the ANSI X.917 standard.

streams are synchronized. Key distribution is a stated assumption, and for the purposes of the ns2 simulation both nodes receive the same initial seed. Should a HELLO message be dropped, it would be noticed at the receiver as packets are expected within a two second window. A missing message corresponds to a delay of greater than two seconds plus a reasonable tolerance factor as discussed further in the results section. The receiver would then decide to increment its key position under the assumption the message is lost. Should messages be potentially altered, assuming the covert channel is known, it would become apparent through the increased error rate or statistically larger noted values of T_A . This is further examined in the results section.

After completing the proof of concept of being able to simulate a covert channel through the manipulation of the jitter values, it is important to examine the distribution of T_A since it is the key factor impacting capacity and wormhole detection. Further experiments are conducted varying potential delay factors through additional CSMA/CA backoff or processing delay within the simulation. Delay values (for T_A) generated by ns2 are written to a text file, parsed with the AWK scripting language and converted into space delimited format for import into Microsoft Excel. Having isolated channel noise, T_A , the parameter associated with determination of channel capacity, it is then possible to study its effects by using MATLAB explained in Section 5.3.

5.2 Wireshark and Tcpdump

A software tool is required that is capable of recording network packet traffic, used to measure timing delay between successive HELLO messages as seen using the Exata emulation software or when using the actual test bed scenario. Two software tools are chosen for this task. Most standard Linux distributions have the `tcpdump` command

precompiled with their kernel. TCPdump is able to record all packet traffic, including HELLO message traffic which can then be saved in a format readable by Wireshark. Wireshark is also able to accomplish the same thing, but presents an easy to use GUI interface, in place of the command line required by Tcpdump. In the experiments involving emulation and test-bed evaluation in this thesis Tcpdump was used to record the required HELLO message traffic which was then further sorted with Wireshark, for expediency purposes.

5.3 MATLAB and Microsoft Excel

Once delay data is captured using ns2 or Tcpdump, MATLAB can be used to manipulate the data and is selected for its extensive library of applicable mathematical functions offering ease of implementation of the previously mentioned Shannon's adapted capacity equations and visual representation tools. The MATLAB workspace allows Microsoft Excel generated tables to be easily imported where they can be manipulated as vectors and arrays.

When importing data captures from the Wireshark packet sniffing program Excel is chosen to format the T_A data and match it to its respective transmitting node, as captured in Wireshark. It was noticed during testing that packets are occasionally dropped in which case the alignment of generated jitter values is affected and must be realigned with their respective node; otherwise key synchronization is lost, making the approach effective against any wormhole attempts to selectively drop HELLO message traffic. It is however relatively simple to deduce this in an implementation as the delay will exceed the expected two second HELLO message interval.

The channel capacity scripts are used to gain an understanding of the channel capacity expected given the distribution of T_A .

Additional MATLAB scripts are used to test various implementations of error correction coding schemes and measure the BER for different data rates. Attempting to replicate the specific error correction coding schemes in ns2 is deemed redundant and without the support of appropriate software libraries, already found in MATLAB.

Another MATLAB software tool used to model the covert channel is the Simulink Real Time simulator with communications toolset. This toolset provided plug and play modules used to evaluate various linear block coding schemes as well as offer a method of visualizing the covert channel generation process. Using Simulink is adequate for smaller coding schemes but difficult to scale to larger coding schemes.

Microsoft Excel is mentioned as it is used to import .csv file format delimited files from Wireshark containing packet timing characteristics. Excel offers simple functionality when sorting packets by nodes and packet delivery timing. Once sorted, Excel formulas discern packet delay intervals at the receiver from which packet jitter is generated. Properly formatted message traffic can then be imported into MATLAB for further analysis. Due to the aforementioned dropped packets it is required to generate a MATLAB script to ensure synchronization between transmitter and sender is maintained.

Any measurements taken in this thesis are based on the limitations of visibility by a receiving node. For example, a receiving node can only ascertain that a packet is dropped based on measurements of delay between successive packets or abnormalities of noise between expected jitter range and measured jitter.

5.4 Exata Cyber Emulation

Exata is a software-based simulation and emulation platform that offers an additional testing capability for the transmission of HELLO message traffic over an OLSR protocol implementation. As promoted in [48] Exata offers an increased fidelity in emulated test beds compared to simulation and is capable of operating in real time with actual physical networks via the use of its Software Virtual Network (SVN) capabilities. Although publications using the tool are sparse in comparison to the known and highly documented ns2 simulator, Exata has already been utilized to demonstrate the effect of wormholes on MANETs in [49].

Exata Cyber version 1.1 is utilized as compiled for the Linux CentOS distribution to test the effects of message delay on the OLSR control channel. Exata offers both OLSR INRIA and OLSRv2 protocol implementations. At present OLSRv2 is still in draft form [50] and this thesis concentrates on OLSRv1 implementations. Specifically, the OLSR version created by INRIA (www.inria.fr) is included with Exata. The OLSR source code from INRIA (version 0.99.15) uses a MAXJITTER variable, used to determine HELLO message jitter, limited to 0.1s as opposed to the 0.5s as per [4]. This can be attributed to the fact that as the OLSR standard does not strongly enforce the use of a strict MAXJITTER variable, from the use of “should” as opposed to “must”, it is not required that a specific implementation of the protocol adhere to 0.5s jitter. The impact is that a lower jitter value will serve to reduce the symbol space, calculated from T_Q .

In order to gain an appreciation for the effects of T_A on OLSR traffic, it is required to modify the source code of the Exata 1.1 software to output the randomly chosen, uniformly distributed values for HELLO message jitter to an output text file. These

values are used internally to set the transmission delay timers, as part of the OLSR protocol, designed to ensure minimal collisions with competing nodes. In the operational and covert use of OLSR HELLO message traffic, the same randomly selected jitter values can be replaced with a cryptographically strong generated sequence as discussed in the ns2 configuration. This sequence then becomes keyed covert message traffic. As this process has already been proven and demonstrated in ns2, it is left as an engineering specific implementation. The predominant independent variable impacting covert transmission is the distribution of T_A which is the focus of the Exata emulation.

Exata allows two separate modes of operation; simulation and emulation modes. Emulation functions in real-time and allows the user to select a virtual interface which is visible to the operating system as is any other interface. The virtual interface can be monitored by any packet sniffer program (Tcpdump or Wireshark), in this case Tcpdump is used to record all OLSR HELLO message traffic as well as write all message traffic to a .pcap file format for confirmation in Wireshark. Wireshark allows for $1\mu\text{s}$ resolution as seen in Figure 16. The original assumption of $20\mu\text{s}$ is retained as it is a standardized measure. Also observed is the expected HELLO interval of 2.0 seconds used in determining the remaining unknown jitter, T_A . It can be seen that Wireshark is able to achieve $1\mu\text{s}$ resolution as seen from the six decimal places recorded in the packet timestamp as shown in Figure 16 under “Time”.

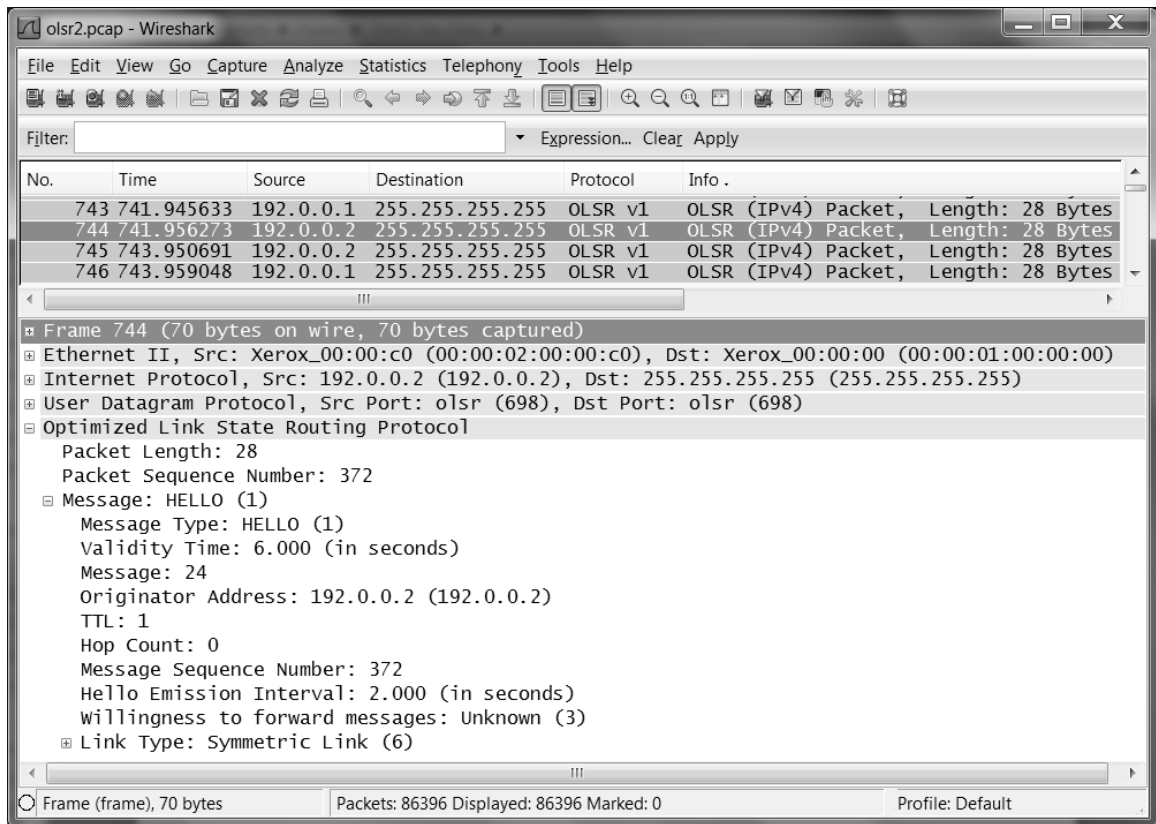


Figure 16: Exata Wireshark Capture

The experiment consisted of an x86 Intel Pentium Core Duo Laptop running Exata 1.1 emulating two nodes with statically assigned IP addresses of 192.0.0.1 and 192.0.0.2 as per Figure 16. No traffic, other than OLSR specific is present in order to gauge the maximum potential for the covert channel under ideal conditions. This is done to examine the highest possible throughput of the system. Within the provided Exata source code files, it is possible to utilize C++ streams to output the jitter value along with the associated node identifier to a text file for each transmitted HELLO message. The experiment is run for approximately 24 hours, which recorded approximately 86400 packets as seen in Figure 16 with half coming from each node every 2.0 seconds.

As Exata is operating in real-time using simulated aspects of virtual hardware with actual processing delays associated with network traffic it displays two clocks

during run time. The first represents the clock associated with the emulation; the second is the actual system clock. Assuming the emulation is running correctly these clocks should always stay synchronized. From inspection, synchronization between the emulation and real-time clock is maintained within ± 2 seconds.

The resulting packet capture traffic is exported to Microsoft Excel in .csv delimited format and aligned with the recorded jitter values as utilized by each respective node. As confirmation the number of captured jitter values is approximately equal to the number of transmitted HELLO message traffic with the difference being HELLO messages that were dropped or not captured.

5.5 OLSRd

The OLSR daemon (OLSRd) is an implementation of the OLSR routing protocol for use under a Linux operating system for Ad hoc networking between computers; it was developed by Andreas Tønnesen as part of his master's thesis [51]. It is available under a Berkley Software Distribution (BSD) license making it openly available for use as a testing platform for covert message traffic analysis. It has since been further developed by the community to version 0.6.1 used in this experiment. OLSRd has been evaluated against ns2 in [52] with noted discrepancies between a real world test bed scenario testing and ns2 simulation, particularly with respect to dropped packets and interference making it a suitable predictor of the potential limitations of covert message passing in a real world instantiation, versus a closed simulation or emulation as previously discussed. As promoted in [51] OLSRd offers low CPU and memory usage thought to minimize the associated delay overheads that contribute to a higher T_A , which negatively affect covert channel and wormhole detection performance.

The purpose of the following experiment is to add real-world factors to an implementation of covert message traffic passing over OLSR ad hoc protocols. Although Exata offers emulation capabilities, a test-bed scenario helps to quantify the expected real world aspects of this analysis.

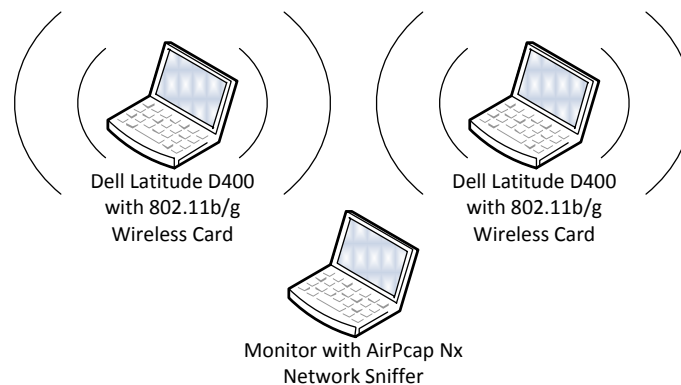


Figure 17: OLSRd Experimental Configuration

The experiment consists of two laptops in close proximity (<1m) as depicted in Figure 16. The two Dell D400 Laptops are configured with a Fedora variant of Linux running OLSRd version 0.6.1 creating an ad hoc network called MONITOR. Each Dell D400 has a local instance of the Tcpdump packet sniffer listening on its wireless network interface. OLSRd is re-compiled with custom additions to enable jitter values, limited by $MAXJITTER = 0.5s$, selected for the transmission of HELLO message traffic to be written out to a file. The third laptop is used to monitor background noise and offer additional packet sniffing capabilities, however it is noted that the AirPcap Nx wireless sniffer does not recover all of the transmitted messages between both nodes. For this reason it was decided to sample only the message traffic at each node's local wireless interface as captured by Tcpdump. As measured by the third laptop and seen in Figure 18 there existed 23 additional access points (APs) within range of the experiment and in

conflict with the established MONITOR ad hoc network utilized by OLSRd.



Figure 18: Interference from External APs on OLSRd Experiment

Given the measured noise present in the system two sub experiments are undertaken. The first is that outgoing message traffic is measured at the local interfaces from each transmitted OLSRd node. This is in addition to the incoming traffic recorded at each node. This is done in preparation to compare jitter noise caused only by the transmitter to jitter noise from both the receiver and transmitter and is discussed further in the relevant results section. Additionally, in order to factor in potentially increased jitter noise resulting from additional CSMA/CA related back-off from constantly busy/noisy channels, an additional experiment is conducted with a single laptop operating as a stand-alone. The node is placed in an environment with no measureable interference from other sources operating in the IEEE 802.11 frequency band.

6 Chapter: Results

In this chapter the theory presented in Chapters 3 and 4 is re-enforced through simulation, emulation and test-bed scenarios as explained in Chapter 5. First, the covert channel is modeled using ns2 to gain an understanding of the noise. The covert channel noise model is then used to predict theoretical channel capacity using the equations from Section 3.2 as well as offer a baseline of channel error rates. Receiver detection theory and error correction coding are then applied and shown to offer improvements in terms of reduced error rates and metrics for wormhole detection. Lastly, additional noise models using Exata and OLSRd are examined as a means of comparison.

6.1 Modeling the Covert Channel with Ns2

In this section ns2 is used to generate the noise, T_A , for both the non-wormhole and wormhole cases over OLSR using constant bit rate (CBR) traffic between nodes. Channel capacity is then examined in the context of these models and under variable SNR. The model in Figure 15 is then applied to improve channel reliability and present a mechanism for wormhole detection.

6.1.1 Covert Channel Noise Model

Using 10^6 samples of T_A as collected from ns2 from two separate scenarios were simulated: with and without the presence of a wormhole. This gives the following probability density functions (pdfs) shown in Figure 19 and Figure 20. The pdf of T_A models the noise present in the channel and all methods examined further in this chapter are directed towards minimizing the effects of noise from T_A on the system BER.

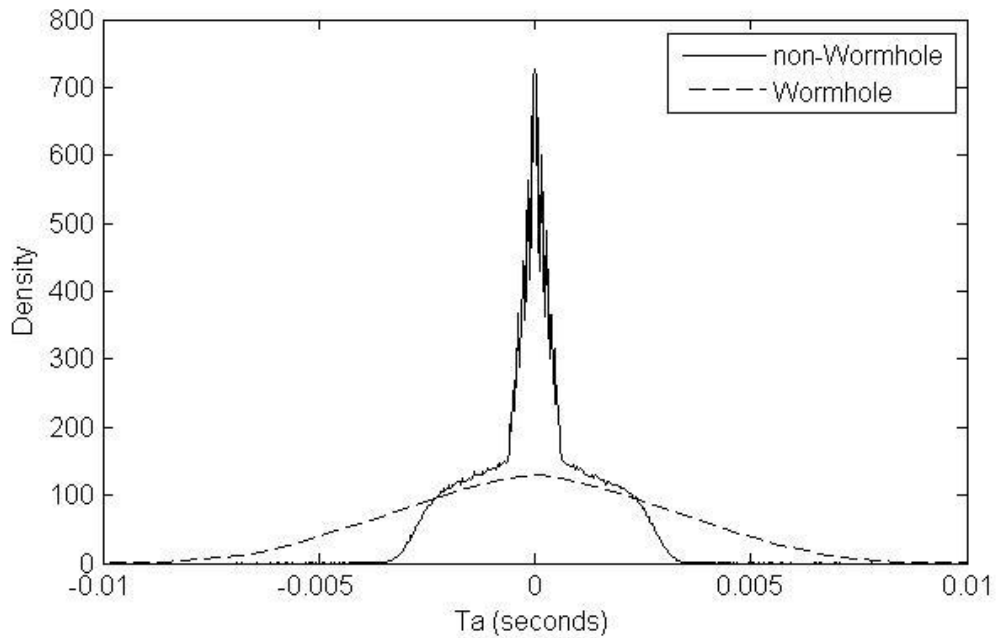


Figure 19: T_A Probability Density Function

From inspection, the distribution of T_A without a wormhole gives a smaller variance than when a wormhole is present. The increased variance of the T_A distribution is expected to contribute to larger bit-error rate (BER) from the channel allowing for a method of detecting the wormhole.

Through the examination of the pdf of T_A , as measured in the presence of a persistent wormhole, it is possible to fit a normal distribution with $\mu=0$ and $\sigma=3e-3$. The distribution can be seen in Figure 20, which conforms to the Normal distribution, consistent with the results in [5].

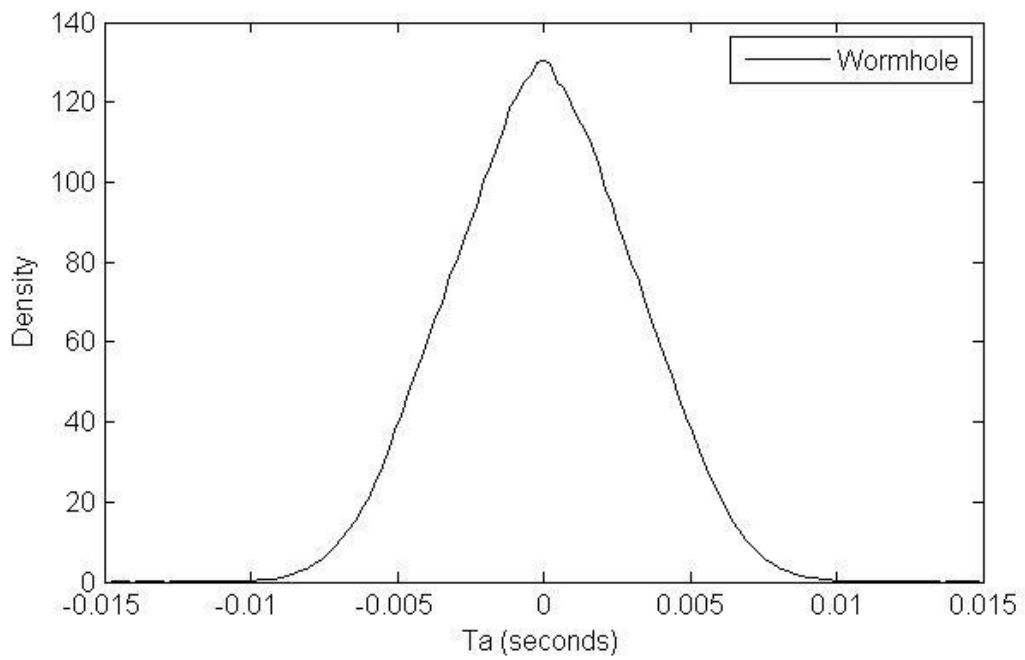


Figure 20: T_A Probability Density Function with Wormhole Present

6.1.2 Measuring Channel Capacity

In reference to the study of capacity, C , from Section 3.2.2, it is possible to plot values of C for different symbol sizes N . A larger symbol encoding will decrease the value of T_Q , in Equation 17.

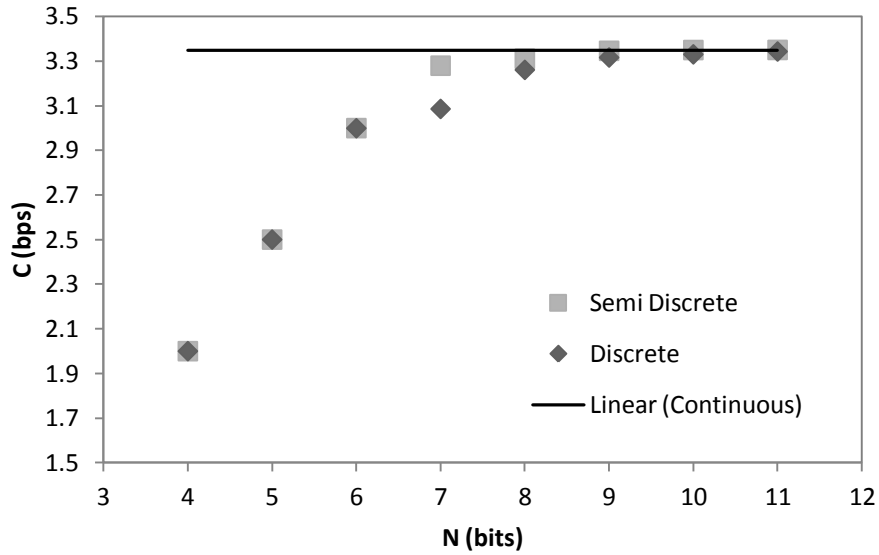


Figure 21: C for various N bit symbols without Wormhole Present

Shown in Figure 21 are the computations of Shannon’s channel capacity equations as applied to the covert channel from Equation 13, Equation 14 and Equation 16 using the noise model from Section 6.1.1 for the non-wormhole scenario. Note that Equation 16 represents the theoretical continuous capacity (assuming the receiver and transmitter have no quantization at all) and is independent of symbol size, N . As such it is represented as a solid line revealing the theoretical ceiling across all symbol sizes shown.

From inspection it is seen that for $N > 8$ bits there is little gain in capacity for increased symbol sizes. Symbol sizes with, $N < 7$ offer roughly linear gains in capacity which begin to reduce at $N = 7$ bits. For these reasons it is possible to conclude that there is little gain, in terms of increased channel capacity, for symbol sizes of $N > 8$ bits in this system.

Repeating the same process when applying the effects of a wormhole gives the results presented in Figure 22.

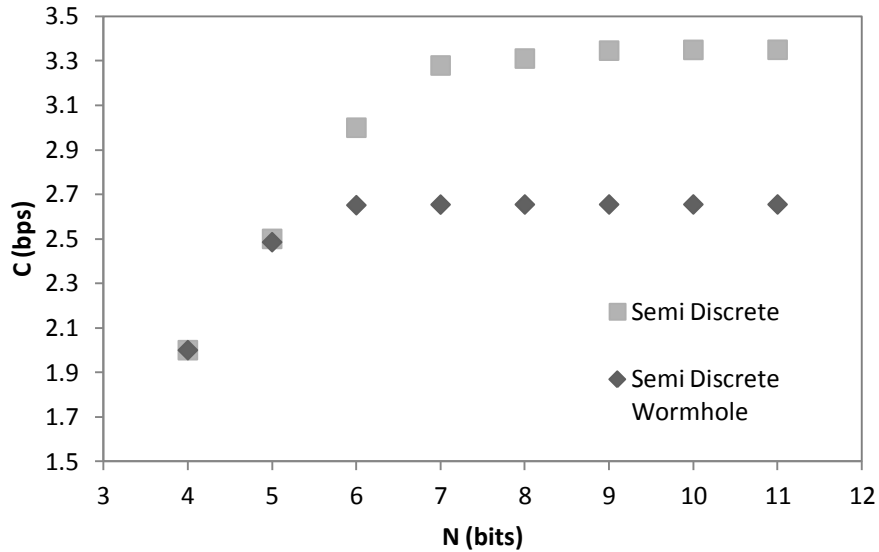


Figure 22: C for various N bit symbols with/without Wormhole Present

From Figure 22 it is possible to observe the direct effects the wormhole has on the system through the reduction of the maximum potential capacity of the channel. This shows that a wormhole should be detectable by observing the degraded performance of the covert channel. Of note is that this form of detection is only possible by using $N > 5$ in the context of this scenario. For smaller values of N , the wormhole provides an insufficient amount of noise to cause a discernible difference in channel capacity.

6.1.3 System Testing under Variable SNR

This section studies the effects of increased SNR on the measured capacity, C from Section 3.2.2. In order to gain insight into the best N -bit symbol selection it is possible to compare the maximum theoretical capacity, from Equation 14 against measured SNR across multiple selections of N . This is accomplished using ns2 to simulate decreasing SNR, achieved through increased noise in T_A , as per Equation 17. There exist two ways to accomplish this in ns2: the first being to decrease the framing size, causing more transmissions, and the second being to increase the node count. Both

methods allow for more collisions in the system which lowers the measured SNR. Four separate experiments are run using ns2 using 10 nodes and varying bit rates of 0kb, or no traffic, 10kb, 50kb and 100kb in order to represent four independent measures of Capacity vs SNR for a given mapping, N between two adjacent nodes. The results are shown in Figure 23 for different mappings of N . Through observation of the results an upper limit of 4.5bps is approached and as N is increased beyond 10 bits, this yields no significant improvement beyond 4.5 bps.

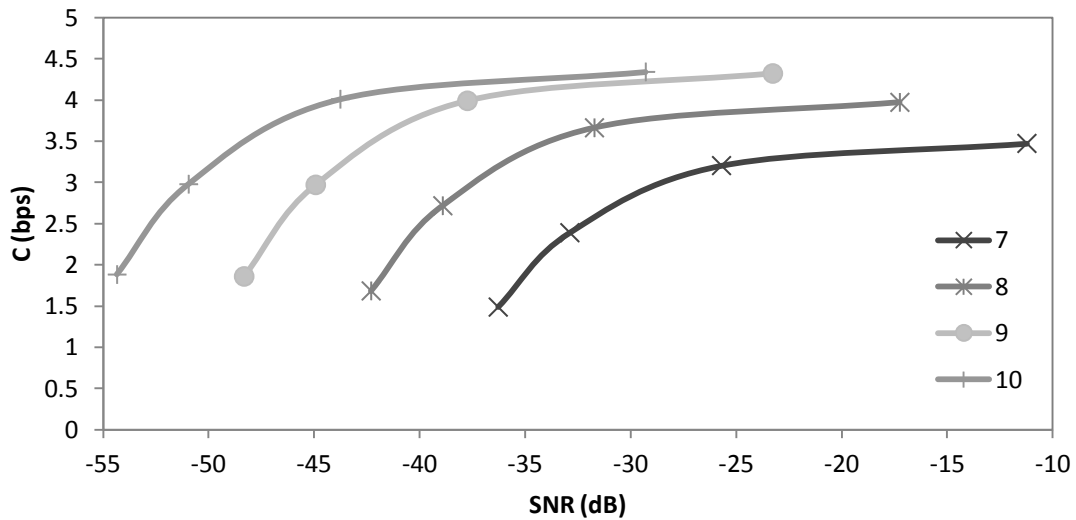


Figure 23: Capacity vs SNR

By using information about the distribution of T_A (e.g variance) it is possible for a node to pre-compute an assessment of the environment when it is added to the network. It can measure channel SNR from T_A , as measured from HELLO message traffic received from other nodes. It can then select the appropriate N -bit symbol mapping based on the computed channel capacity. As HELLO message traffic is only point to point it is possible for nodes to harmonize symbol selection schemes using this method. Given a nodes' understanding of the measured noise, T_A , it is possible to select the appropriate coding scheme to reduce the measured BER in the channel.

With respect to wormhole detection using variance as discussed in [3], the topic of T_A , or channel SNR brings about an important point. As more traffic or nodes are brought into a system the variance of T_A will inevitably increase. It becomes important to ensure that this increase is not mistaken for wormhole presence. For this reason it becomes important to consider multiple factors, aside from variance, in predicting wormhole presence along with ensuring appropriate thresholds and expected environmental operating parameters are thoroughly tested.

6.1.4 Evaluating Channel Error Rates

In this scenario ns2.34 is configured with 2^N symbols, where N is the number of bits used to encode each of $M = 2^N$ symbols. The first scenario uses a system of two nodes transmitting 2Mbps constant bit rate (CBR) traffic in ns2. The results of N -bit symbol size to bit error rate (BER) for both wormhole and non-wormhole traffic are presented in Table 1. The wormhole is modeled, as per Figure 20, and based on the assumptions, from Equation 5, and is added to give an indication of the increased error rate associated with the addition of wormhole delay.

N	BER	BER (Wormhole)
4 Bit	< 2.5E-07	< 2.5E-07
5 Bit	2.0E-07	0.0030
6 Bit	5.2E-05	0.0713
7 Bit	0.0485	0.1518
8 Bit	0.1041	0.1996
9 Bit	0.1350	0.2341

Table 1: Ns2 Observed BER using Simple Binning

BER is measured from simulation by modeling T_A using 10^6 captured samples from ns2.34 with known message traffic. It is possible to determine the value of T_A using

Equation 4. The values of T_A are then extracted from ns2 and inputted into a MATLAB Simulink model, as well as a MATLAB script. Upon inspection, it appears the effects of BER, per increased values of N , are relatively low until 7-bit symbols are used after which the BER increases. This is because the noise, modeled with T_A , is not sufficient to cause errors in the channel until $N = 7$. When the same simulation incorporates a wormhole the observed BER increases as symbol size, $N > 5$, increases as shown in Table 1. This agrees with the results of capacity computations, as shown in Figure 22, after $N > 5$ there is a significant divergence in terms of calculated channeled between wormhole and non-wormhole capacity, which amplifies why BER is increasing.

Another metric of performance to consider when evaluating the covert channel is Symbol Error Rate (SER) as pertaining to the number of symbols, vice bits, received in error of a message. If one or more bits are in error, the entire symbol, consisting of N bits, is malformed. This impact is amplified in the case of the larger N -bit symbol sizes. The SER for both the wormhole and non-wormhole case is given in Table 2. The mapping in this case is only straight binning of values to $M = 2^N$ possible symbols.

N	SER	SER (Wormhole)
4 Bit	<1.0E-06	<1.0E-06
5 Bit	1.0E-06	0.0076
6 Bit	1.5E-04	0.2173
7 Bit	0.1713	0.5359
8 Bit	0.4170	0.7537
9 Bit	0.5738	0.8742

Table 2: Ns2 SER using Simple Binning

Channel throughput, T , is used to define the average amount of successfully received information, in bits/second [53] [54] based on symbol size, N , per HELLO message interval, K (2 seconds). This is shown in Equation 27 as a means to contrast measured throughput to the theoretical capacity of the channel. Channel throughput is half the symbol size in bps.

$$T = \frac{N}{K} \text{ bits/s}$$

Equation 27: Throughput

For the 2Mbps CBR channel, the non-wormhole channel capacity is 3.3 bps, calculated from Equation 16, and shown as the solid line in Figure 21. Intuitively, for the distribution of T_A , given in this example, the focus of coding efforts is chosen to be on the $N > 6$ symbol length cases where BER is significantly higher and where the system approaches capacity. An additional property to note is that the BER in the case of wormhole is much more pronounced at $N=6$ and $N=7$ -bit symbol lengths. This will have additional bearing when examining methods of wormhole detection.

It is observed, using Figure 21, that throughput, T , operates near Shannon's theoretical maximum capacity, from Equation 16, until $N=7$ bits or greater. Efforts are therefore focused on increasing throughput for the $N > 6$ cases.

It can be seen that in the case of the presence of a persistent wormhole, after bin sizes of $N = 5$ bits the BER increases substantially, in Table 1, indicating that 5-bit is the best possible, in terms of throughput at low BER, when only using simple binning. Without the presence of a wormhole larger bin sizes can be used up until $N = 6$ -bits before BER increases significantly. The decision could be taken at both the receiver and transmitter to adjust bin sizes based on the detected presence of a wormhole to ensure

that error free and maximally efficient communication persists. Also of note is that 4-bit sized bins are impervious to both wormhole and non-wormhole based traffic, but to simply select 4-bit bin scheme would be inefficient in terms of a potential maximization of throughput. Also the choice of using $N=4$ doesn't allow for wormhole detection using the schemes presented in this thesis as it offers no change in BER.

Another possible method to examine the effects of a wormhole comparatively against standard traffic transmission is to examine the distribution of T_A as seen by the receiver. Using the same situation, of a persistent wormhole, as previously discussed the probability density function (pdf) of T_A with and without a wormhole are shown in Figure 19 and Figure 20.

Comparing the initial results in Table 2 against the measured outcomes in [8] offers reduced BER at increased throughput. For example, [8] offers a maximum throughput of approximately 2 bps with a probability of loss over 20%, using AODV, contrasted against ~3 bps with a BER of 0.01% using 6 bit symbols from Table 2 converted to units of bps. Even though the bit rate is perhaps comparable, the distinguishing factor is the reduced BER offered using OLSR. Owing to the fact that the approach taken in this thesis is fundamentally different than [8], in order to better compare the results from [8] against the results discussed here the models need to be compared over various levels of SNR for which data is not included from [8]. Given the lower BER presented here, it is anticipated OLSR covert methods will fare better in the presence of increased noise.

6.2 Improving the System Through Application of Receiver Detection Theory

Now that the channel noise model, capacity and error rates have been measured, this section examines improvements to the covert channel using receiver detection methods previously introduced in Chapter 3. The approach is to examine each method independently to gauge its value and combine all effective methods in future scenarios for maximum results.

6.2.1 Maximum likelihood Symbol Detection

As discussed in Section 3.3.1 the use of Maximum Likelihood Symbol Detection (MLSD) can be employed by the receiver, given an understanding of the expected distribution of T_A to more accurately predict the symbol received. This is accomplished by maximizing the probability, $P(y|x[j])$, where y represents the symbol received, limited to the sensitivity of the receiver ($20\mu\text{s}$, as per assumption) and $x[j]$ is the intended discrete symbol transmitted in the range of 2^N possible symbols with a N -bit mapping scheme used. In the context of the hard decision process implemented from the covert model, shown in Figure 15, maximizing $P(y|x[j])$ is accomplished by using a minimum distance detector to the nearest bin. Therefore MLSD is integrated into the symbol decoding process already in this thesis.

6.2.2 Gray Mapping

Gray Mapping is a method of maintaining a one bit Hamming distance between adjacent symbols. As MSLD is targeted towards reducing pre-error corrected symbol errors, the advantage of Gray Mapping is that it reduces the resulting bit errors assuming they result from mistakenly detecting an adjacent symbol. The results of adding Gray Mapping with and without the presence of a wormhole using the same distribution of T_A ,

are shown in Table 3. The delta (Δ) represents the difference between BER with the method and without. A negative value indicates a reduction in BER.

No Wormhole	BER	Δ	Wormhole	BER	Δ
4 Bit	< 2.5E-07	N/A	4 Bit	< 2.5E-07	N/A
5 Bit	2.0E-07	0.0000	5 Bit	0.0015	-0.0014
6 Bit	2.5E-05	0.0000	6 Bit	0.0362	-0.0350
7 Bit	0.0245	-0.0240	7 Bit	0.0845	-0.0674
8 Bit	0.0538	-0.0503	8 Bit	0.1390	-0.0607
9 Bit	0.0957	-0.0393	9 Bit	0.1796	-0.0545

Table 3: BER using Gray Mapping

From inspection of Table 3 it can be seen that Gray Mapping reduces BER compared to the non-Gray Mapped case shown in Table 1.

In order to ascertain the results of the additive effects of Gray Mapping on the Symbol Error Rate (SER) the same scenario is considered. With the application of Gray Mapping there is little change in SER as symbols are still decoded in error as long as there is at least one bit error present and there exists no error correction. Having more or less bit errors per symbol does not affect the SER in the case of Gray mapping only. This is visually summarized in Figure 24 and Figure 25 with and without the presence of a wormhole. As observed, the presence of a wormhole increases BER and SER as measured by the receiver and Gray Mapping offers a reduced BER in both cases.

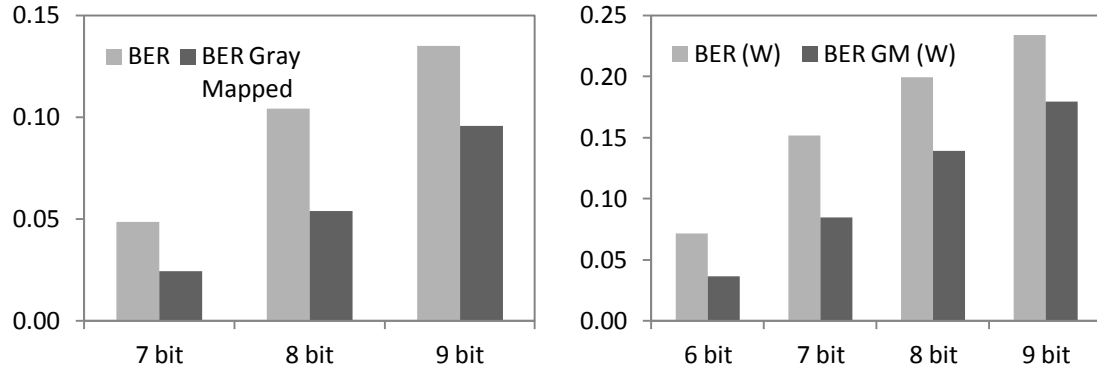


Figure 24: BER without and with a Wormhole

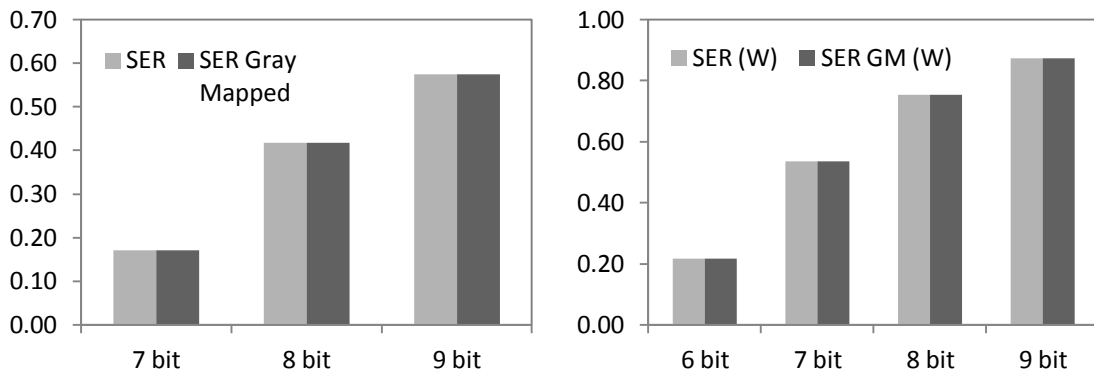


Figure 25: SER with and without a Wormhole

6.3 Improving the Model with Error Coding Theory

Now that the pre-error coded symbol related errors have been reduced with the applied methods from the previous section error correctional coding are now applied in order to further reduce BER and increase channel reliability.

6.3.1 Linear Coding Schemes

This section applies the principles of linear block coding theory, as discussed in Section 3.4.1, with different code sizes and reports the effects on BER and throughput. BCH codes are selected, given their widespread use and ease of decoding by the receiver therefore minimizing the potential effects on hardware complexity. Given the positive

results, Gray Mappings are automatically integrated into the linear coding schemes in order to reduce BER.

The approach taken is to apply the coding scheme, implemented using BCH codes in MATLAB, with the T_A distribution recovered from the ns2 simulation for with and without the additional channel noise added by wormhole re-transmission. MATLAB is used to generate random message traffic. The value of N chosen determines the number of bits per symbol from Equation 8.

The value associated with n here is the length of the BCH code, k is the message length and $R = k/n$ is the code rate, as discussed in Section 3.4.1. Given selected values for n and k a series of blocks of data are created to accommodate the BCH(n,k) code with the selected N -bit message encoding scheme, which is also Gray Mapped to ensure minimum Hamming distance between adjacent message symbols. The resulting BCH(n,k) code block is sequentially transmitted, using N -bit symbols, with the noise from the T_A distribution added. At the receiver, the BCH(n,k) code block is reassembled and decoded. It then becomes possible to compare the received and transmitted message blocks at both the bit level (for BER calculation) and message symbol level (for SER calculation). T_{eff} , shown in Equation 28, represents effective throughput. With code rate, R , and HELLO message interval, K (2 seconds per HELLO message), effective throughput is given by:

$$T_{eff} = \frac{RN}{K} \text{ bits/s}$$

Equation 28: Effective Throughput

In examining the BER results from Table 1 and Capacity results from Figure 21, values of $N=7$ and $N=8$ are selected as a starting symbol sizes in order to evaluate an

improvement in BER using linear coding, given their higher BER when using the simple binning procedure. These selections offer a balance of minimizing the effects of noise from T_A while offering larger channel capacity.

For the noise model shown in the shortest code length possible is a BCH(7,4) code with $N = 7$ bits which can be decoded after one HELLO message is sent. The corresponding impacts on BER, both with and without a wormhole present, are shown in Table 4. In comparison to the $N = 7$ bit case from Table 1 the results below show an approximate four order of magnitude reduction in BER.

No Wormhole	R	N	N*R	T _{eff}	BER	SER
BCH(7,4)	0.5714	7	4.0000	2.0000	6.00E-06	4.20E-05

Wormhole	R	N	N*R	T _{eff}	BER	SER
BCH(7,4)	0.5714	7	4.0000	2.0000	0.0150	0.0901

Table 4: BCH(7,4) Code for N=7 bit Symbols

Notably, it is possible to achieve a similar BER result by selecting a lower value of $N = 5$ without any coding, but this method does not offer the wormhole detection, through corrected error count information, examined later on.

In an effort to increase T_{eff} while maintaining a low BER BCH codes are chosen so as to present similar BER at increasing code rates. The values of n and k are computed using a BCH code generation tool from [55]. It was not possible to significantly increase the code rate, R , from Table 4 while maintaining the same BER without using code lengths greater than $n = 1023$ bits. Alternatively, Table 5 and Table 6 below offer a sample set of BCH codes, using $N = 7$ and $N = 8$ bits, capable of increasing R at a cost of an increase to the BER.

No Wormhole	R	N	N*R	T _{eff}	BER	SER
BCH(15,7)	0.4667	7	3.2667	1.6333	5.64E-04	2.20E-03
BCH(255,155)	0.6078	7	4.2549	2.1275	3.86E-04	2.62E-03
BCH(511,331)	0.6477	7	4.5342	2.2671	5.54E-04	3.68E-03
BCH(1023,668)	0.6628	7	4.6393	2.3196	4.74E-04	3.19E-03

Table 5: BCH(n,k) Codes for N=7-bit Symbols

No Wormhole	R	N	N*R	T _{eff}	BER	SER
BCH(127,50)	0.3333	8	2.6667	1.3333	5.27E-04	2.47E-03
BCH(255,107)	0.4196	8	3.3569	1.6784	5.16E-04	3.73E-03
BCH(511,220)	0.4305	8	3.4442	1.7221	5.29E-04	3.84E-03
BCH(1023,443)	0.4330	8	3.4643	1.7322	2.89E-04	2.15E-03

Table 6: BCH(n,k) Codes for N=8-bit Symbols

As can be observed, shorter BCH codes offer a lower T_{eff} than longer BCH codes. The tradeoff is the decode time, which is the amount of time to transmit the n bit block code to recover the k bit message. In the case of a BCH(7,4) code this is 2 seconds. Comparatively, an $n = 1023$ code would require ~5 minutes to transmit the entire code block before decoding could occur. A tradeoff exists between time to decode and T_{eff} . Importance is placed on the decode time as the wormhole detector, discussed in Section 6.5, relies on the number of corrected errors. The sooner this information is available the sooner the node can determine the presence of a wormhole.

The results, comparing T_{eff} to decode times, are visually summarized in Figure 26. In order to exceed the effective throughput of 2 bps offered by a BCH(7,4) code larger codes are required at a cost to BER. By trying a larger symbol size of $N = 8$ it is not possible to increase T_{eff} while preserving a similar BER.

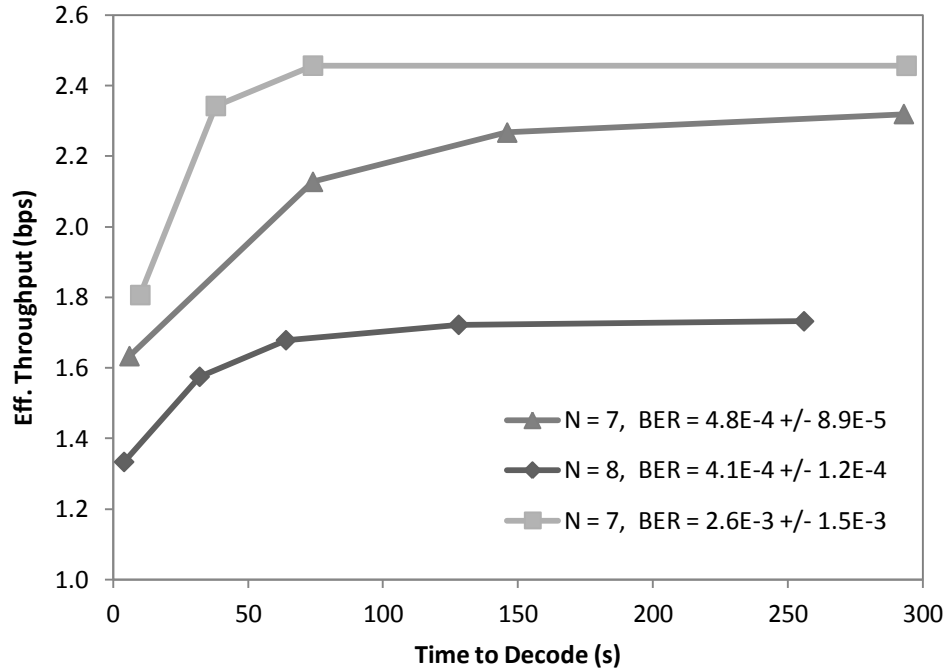


Figure 26: Teff vs BCH Code Decode Time

With the addition of Gray Mapping and BCH Codes at a small cost to T_{eff} it is possible to reduce the observable BER by two or more orders of magnitude, depending on the selected code. This is an important gain from the perspective of the overall channel. With the error rate reduced error correction handling procedures can be minimized at the upper layer. This ensures effective message transfer over the channel given the noise described by the T_A distribution.

In order to observe the effects of a wormhole on the previously shown coding schemes the same experiments are run using wormhole delay traffic. Table 7 shows the results of using the same codes selected from Table 5 when a wormhole is present. As can be seen BER and SER increase in both cases due to the increased noise, T_A . The same trials are repeated using $N = 7$ and $N = 8$, with the results shown in Table 7 and Table 8.

Wormhole	R	N	N*R	Teff	BER	SER
BCH(15,7)	0.4667	7	3.2667	1.6333	0.0251	0.0901
BCH(255,155)	0.6078	7	4.2549	2.1275	0.0834	0.5103
BCH(511,331)	0.6477	7	4.5342	2.2671	0.0841	0.5160
BCH(1023,668)	0.6628	7	4.6393	2.3196	0.0846	0.5182

Table 7: BCH(n,k) Codes for N=7-bit Symbols with Wormhole Present

Wormhole	R	N	N*R	Teff	BER	SER
BCH(127,50)	0.3333	8	2.6667	1.3333	0.1278	0.6759
BCH(255,107)	0.4196	8	3.3569	1.6784	0.1386	0.7409
BCH(511,220)	0.4305	8	3.4442	1.7221	0.1391	0.7485
BCH(1023,443)	0.4330	8	3.4643	1.7322	0.1392	0.7479

Table 8: BCH(n,k) Codes for N=8-bit Symbols with Wormhole Present

In summary error correction coding offers insight into the presence of a wormhole through an observed increase in BER and SER. This will be an important aspect examined later on, in Section 6.5 on wormhole detection. It is noted that in order to reduce the effects of the wormhole on BER and SER higher codes can be chosen by the sender, depending on an appropriate negotiation between sender and receiver.

In order to measure the effectiveness of Gray Mapping the results for error correction are re-examined without Gray Mapping present in the system using a BCH(7,4) code as an example with the BER and SER shown in Table 9.

Wormhole	R	N	N*R	Teff	BER	SER
BCH(7,4)	0.5714	7	4.0000	2.0000	2.99E-02	1.52E-01

Table 9: BCH(7,4) for N=7-bit Symbols, no Wormhole Present and no Gray Mapping

From inspection it can be seen there is a significant impact on the BER, which increases to 3E-2 from 6E-6, as calculated in Table 4. This is attributable to the fact that with a BCH(7,4) code it is only possible to correct one bit error per transmitted symbol.

As Gray mapping ensures at most a 1-bit difference between adjacent symbols it is possible to correct for 1-bit errors resulting from incorrectly interpreting an adjacent symbol to have been received. Without Gray mapping an incorrectly interpreted adjacent symbol that has a Hamming distance >1 bit cannot be corrected by the BCH(7,4) code.

6.3.2 Convolutional Coding Schemes

Convolutional coding schemes offer an additional avenue towards the improvement of the covert channel. One of the advantages is that the decoder does not have to wait for an entire code block to be transmitted and can operate on smaller sets of received symbols. This will be important when considering the amount of time required gathering error statistics at the receiver to determine wormhole presence.

In order to evaluate convolutional coding a series of codes are taken from [56] and implemented in MATLAB⁴. Similar to the linear block code case, a series of random symbols are generated and converted into N -bit symbols in Gray Mapped format. Using a selected convolutional code the symbols are encoded. Noise is added to the channel via the noise modeled by T_A . At the receiver the symbol is then decoded using the Viterbi algorithm [32]. Codes are chosen to reduce the BER and SER while attempting to maximize T_{eff} . Beginning with the non-wormhole case, results are shown in Table 10. As specified in [56], L represents the highest degree of the coefficient polynomials specified in $G(x)$. The variable, d_{free} , represents the minimum distance between any two code

⁴Note for implementing MATLAB convolutional codes using the `poly2trellis` function, MATLAB assumes that padded octal generator coefficients are placed as MSBs, vice LSBs as in [56]. For example, if $L=4$ a value of $g_1=40$ (octal) becomes $g_1=10$ (octal) in MATLAB. This is due to the two padded zeros moved from LSB to MSBs as a matter of notational differences. Values shown here are in MATLAB format.

sequences. Codes with larger values of d_{free} perform better, in terms of error correction at the cost of complexity, generally speaking. The codes examined are below in Table 10⁵.

No Wormhole										
L	G(x)				dfree	R	N	BER	SER	Teff
14	21113 23176 35527 25537				36	1/4	8	< 1.3E-7	<1.0E6	1.000
	9	4.1E-06	2.9E-05	1.125						
	10	4.8E-04	2.6E-03	1.250						
	11	1.0E-02	4.4E-02	1.375						
17	347241		246277		20	1/2	7	6.8E-06	3.3E-05	1.750
							8	1.6E-03	6.0E-03	2.000
							9	1.7E-01	4.1E-01	2.250
							10	4.0E-01	8.6E-01	2.500

Table 10: Hard Decision Convolutional Codes with no Wormhole Present

In order to reduce the observable SER and BER to levels seen in the previous section using linear block schemes, convolutional codes with $R=1/2$ or less were chosen. Compared to the BCH linear block codes from the previous section, convolutional codes are not able to achieve as high of a T_{eff} , using hard decisions, but allow for the use of larger symbol encoding sizes of N with less impact on SER and BER. When R is increased to beyond $1/2$ the BER is greater than the un-encoded case making $R= 1/2$ the highest possible selection for that particular distribution of T_A .

Next, soft-decision decoding is investigated using the techniques discussed in 3.3.4, specifically the Log Likelihood Ratio (LLR), which assigns a probability value to each interpreted bit at the receiver, is employed. A Viterbi decoder with soft decision decoding is able to use the LLR probabilities to determine, with better accuracy, the

⁵ Of note is that some common convolutional code puncture patterns were examined as a means to increase the code rate of $R=1/2$ convolutional codes with negative results with BERs higher than that of the un-encoded case, and were therefore omitted. Potentially, there exists future work in this area.

correct path through the trellis. Improvements in BER for larger symbol sizes, N , with a code rate of $R=1/2$ are shown in Table 11. Larger mappings of N are possible to potentially further increase the observed value of T_{eff} and are left to the designer how best to tradeoff increase BER. In both cases, with and without a wormhole present, BER and SER increase when a wormhole is present implying that convolutional coding can be used as a method for wormhole detection.

No Wormhole									
L	G(x)		dfree	R	N	BER	SER	Teff	
17	347241	246277	20	1/2	8	< 1.3E-7	< 1.0E-6	2.000	
					9	6.3E-05	2.7E-04	2.250	
					10	5.9E-05	2.5E-04	2.500	
					11	7.1E-03	2.7E-02	2.750	

Table 11: Soft Decision Convolutional Codes with no Wormhole Present

A comparison between soft decision and hard decision metrics, in terms of BER for selected symbol sizes, N , is shown in Table 12 with a visibly larger improvement associated with the soft decision process. With both soft and hard decision metrics BER and SER increase in the presence of a wormhole, as shown in Table 13.

In examining the potential tradeoff in terms of comparable effective throughput as observed from the linear block coding schemes a BCH(31,16) code requires 10 seconds (with $N=7$) before BER data can be collected. With convolutional coding there is an initial period required to populate enough information into the decoder before decoding is possible, but after this point error correction is possible after each received symbol. In the scheme utilized in MATLAB with a trace back length of 30 equates to 558 bits or ~2 minutes with $R=1/2$ at $N=9$ from Table 10.

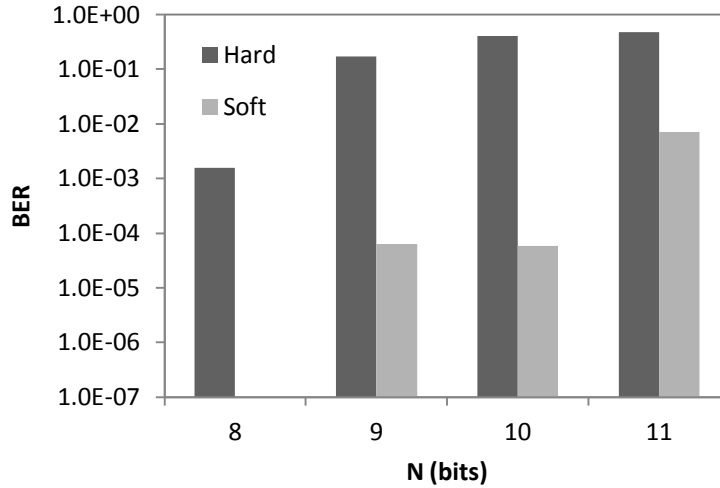


Table 12: Soft and Hard Decision Decoders Compared at R=1/2 codes

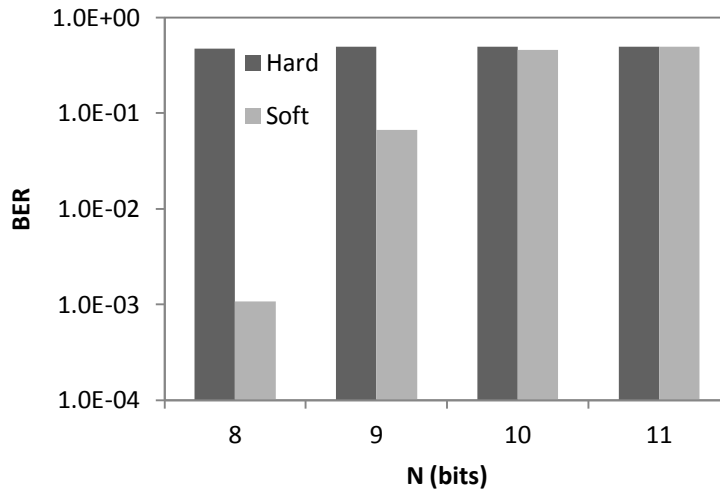


Table 13: Soft and Hard Decision Decoders Compared at R=1/2 codes (Wormhole)

6.4 Covert Channel Detection

In the previous section it was possible to determine the BER over a proposed covert channel. In this sub-section, the various techniques, discussed in Section 4.1 as a means to gain confidence in the stealth capabilities of the channel, are examined.

In a basic cryptanalytic sense the underlying unencrypted covert symbol stream, T_{DJ} , carries patterns depending on the message being sent from the inherent characteristics of a communication language. Should it be directly transmitted without the

keyed jitter, from Equation 4, it would become obvious to an eavesdropper that the jitter contained a message, using the techniques presented in Section 4.1. As a test to evaluate the effectiveness of the keyed jitter technique, using a modulo $K/4$ addition and subtraction, only one specific symbol, T_{DJ} , is sent with random keyed jitter, T_{KJ} , and the resulting distribution as shown in Figure 27 using 100k samples as recorded from ns2.

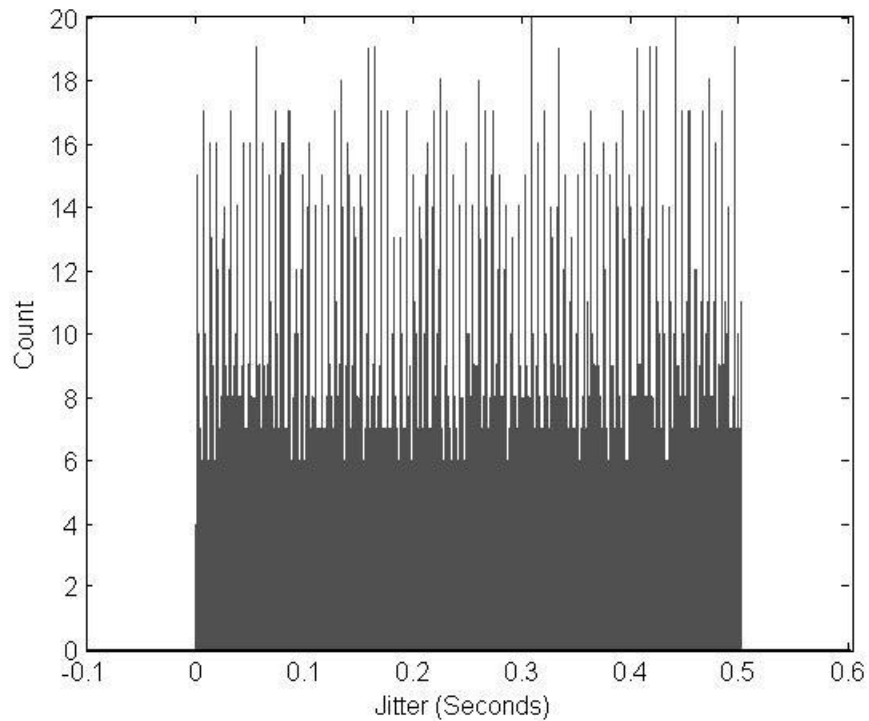


Figure 27: Covert Jitter Distribution

It is demonstrated that even with constant symbol being transmitted the resulting distribution appears uniform between $[0, 0.5]$. Without the addition of the keyed random jitter the distribution in Figure 27 would be a single point which would lead an observer to infer that there is a possibility that covert communication is taking place. In order statistically confirm that the randomness inherent with the keyed jitter scheme is sufficient to mask the deliberate jitter, the Kolmogorov-Smirnov test is applied at a 99% confidence interval against a set of 100k uniformly distributed samples. This is

accomplished in MATLAB with the null hypothesis being that the distributions are the same. The resulting Kolmogorov-Smirnov (K-S) test fails to reject this hypothesis concluding that it is not statistically possible, with 99% confidence, to determine a difference between the distributions created by transmitting a single repetitive symbol against a random uniform distribution as measured by the receiver

The same tests are completed on a distribution of random jitter values with both a constant and random symbol using $N=1$ and $N=10$ bit symbol values added with modulo 0.5s with no change in the results to conclude that a discrete symbol addition to a uniform continuous distribution has no measureable impact on the resulting distribution in a statistical comparative sense.

Finally, the order of received jitter values is examined so as to ascertain if the ordering is in fact random or subject to a pattern as studied in [33]. This is accomplished using the `runtest` and `signtest` functions from the Statistical Toolbox included in MATLAB at 95% confidence levels which also fail to reject the null hypothesis thereby concluding that even with non-random symbol traffic over the covert channel it is possible to create a random pattern of jitter values resistant to the methods employed in this thesis.

In order to characterize the improvements of using additive keyed jitter against the XOR'ed message scenario, presented in Section 3.1.1 and from [15], consider the following example. The covert message, *msg*, is "hello". After conversion to hexadecimal (ASCII coded) format symbol set, *S*, it is XOR'ed with keyed jitter set, *J*, resulting in *S'*. Assuming 4-bit symbols, the binary message shown below in Figure 28 is transmitted in symbols of four bits.

```

msg = hello
S = 0x48 0x65 0x6c 0x6c 0x6f
J = 0xfc 0xd2 0x13 0x47 0x32 ⊕
-----
S' = 0xb4 0xb7 0x7f 0x2b 0x5d
    1011 | 1011 | 0111 | 0010 | 0101
    0100 | 0111 | 1111 | 1011 | 1101

```

Figure 28: Discrete Keyed Jitter Example

Although confidentiality of the message is assured through the XOR operation with the key values, J , the resulting discrete values, if simply sent over the channel, result in “discrete-like” jitter distribution vice the continuous distribution presented in Figure 27. This can be shown by selecting $N=4$ bits in line with the example in Figure 28 above. The resulting distribution with the noise from T_A is shown in Figure 29.

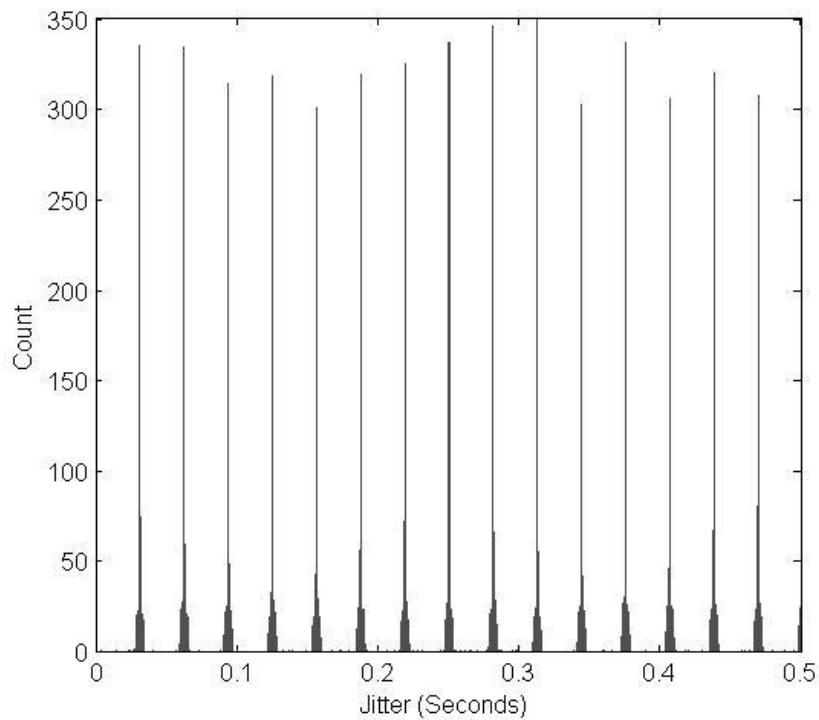


Figure 29: Discrete Jitter Values with Noise T_A

It is visually possible to observe a different distribution. When applying the K-S test the null hypothesis is rejected at a 95% confidence interval proving the distributions are statistically distinguishable. As a test the value of N is increased with negative results until $N=8$ -bits at which point the K-S tests fails to statistically observe a difference between the discrete jitter distribution and the uniform random case. This implies that a minimum 8 bit coding scheme is required when using the XOR method, which as shown earlier carried an BER of 11%, from Table 1, which is an unacceptable level of error (unless combined with an error-correction code).

In summary, for both cases, the additive jitter offers advantages in channel stealth, but comes at the cost of increased BER from symbol wrap-around, as discussed in Section 4.1. The choice of cryptographic algorithm and any associated weaknesses are not considered here as the encryption chosen is a function of the security required. A noted difference in a case of cryptanalysis with respect to the covert channel as implemented here is that jitter traffic is a standard product of the system and is created even when no covert message is sent. This makes it difficult, in cryptographic terms, to separate cipher text from random jitter.

6.5 Wormhole Detection

As presented in various sections, the inclusion of error correctional coding methodologies allows for an elegant strategy to detect wormholes. As seen in Figure 24 in the case of straight binning it is possible to observe increased BER and SER when a wormhole is present. Although straight binning offers a slightly higher throughput, T_{eff} , in order to measure BER and SER a known message sequence has to be sent meaning that no actual communication is taking place.

The advantage of using forward error correction (FEC) schemes, such as block coding and convolutional coding as presented in Section 6.3.1 and Section 6.3.2, allow an observed BER and SER to be calculated by the receiver using the inherent redundancy in these schemes without the need for known message traffic. The fundamental difference between the two mentioned coding schemes being that with block coding the receiver needs to wait until the entire block, of n bits for a (n,k) code, is received before estimating error. A BCH(7,4) code can produce actionable results, through corrected error count, after 2 seconds with symbols size $N = 7$ bits. With larger block codes, such as a $n = 255$ code this can be ~ 1 minute with $N = 7$ bits. The key is to select the appropriate code to the required application, which will be an iterative process.

To illustrate with an example, using the T_A distribution from Figure 19, a BCH(7,4) code has an observable BER of $6e-6$ with symbol size $N = 7$ bits, as seen from Table 4. Using these same parameters the additional delay for a Rayleigh distributed ($\sigma=0.002s$) wormhole gives a BER of $1.5e-2$. The measured error rates presented so far represent the absolute error, given the original message is known. In actuality the receiver will not be able to compare its decoded message to the original message and is limited to the observable errors as determined by the decoding process (i.e. the receiver will know how many errors it corrected). The receiver has to make predictions on whether or not a wormhole is present based on the number of corrected errors from the FEC scheme which could be different from the actual number of errors present in the code block. Another question to answer is at what point, or confidence level, can an accurate prediction of a wormhole be made through examination of the corrected errors determined by the

receiver during the decoding process. With each successive decoding operation the FEC confidence will increase with increased sample size.

An experiment is conducted in order to gain insight into how coding theory can be used for wormhole detection. It assumes a BCH(7,4) code with $N = 7$ offering a more expedient method for which to calculate corrected error statistics compared to the codes examined previously, at the cost of a lower code rate. It is then possible after $\frac{n}{N}K = 2$ seconds (n is code length, N is symbol size and K is symbol period) to examine the number of corrected errors at the receiver. The experiment consists of examining the samples from the ns2 T_A distributions, for both wormhole and non-wormhole cases, used in Figure 19 to create a series of 500,000 randomly chosen sets of ten sequential samples with and without a wormhole present. The number of receiver detected errors are cumulatively summed from each the ten samples. The ability to predict that a wormhole is present is determined by examining the difference in cumulative error counts between wormhole and non-wormhole present cases, whereby an error-count threshold can be established with a given confidence interval. Examining the cumulative corrected error count using the T_A distribution up to 10 consecutively transmitted $N = 7$ bit symbols with a wormhole present is summarized in Figure 30 using a box plot showing the distribution, in terms of each quartile at a specific decode of the code block. For example, after four code blocks are transmitted, the 50th percentile shows that two errors in total are present.

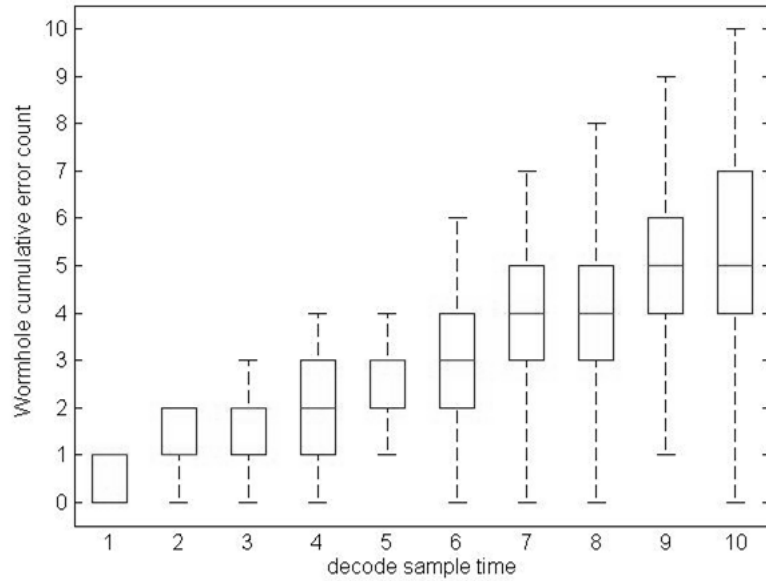


Figure 30: Wormhole Detection Statistics

On observation of Figure 30 it can be seen that in the case of a wormhole the median number of receiver observed cumulatively corrected error counts trends upwards with each successively received symbol. In contrast, the median value for the case when a wormhole is not present increases at a lower rate, as shown in Figure 31.

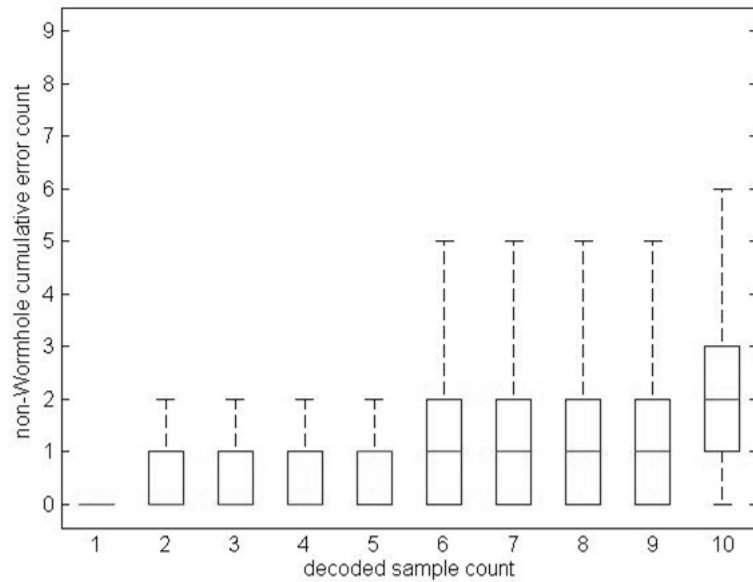


Figure 31: Non-wormhole Detection Statistics

A method for determining an error-count threshold level after k code block samples (of length n) are received, denoted $T[k]$, is established by determining the middle point between the average number of errors corrected after k samples with and without a wormhole present. A table of computed $T[k]$ values for both cases is shown in Table 14.

k	Wormhole	Non-Wormhole	T[k]
1	0.5349	0.1709	0.3640
2	1.0725	0.3425	0.7300
3	1.6075	0.5137	1.0938
4	2.1426	0.6841	1.4585
5	2.6789	0.8547	1.8242
10	5.3576	1.7153	3.6423

Table 14: Mean Cumulative Error Counts

In order to establish a confidence interval with respect to correctly determining if a wormhole is present; two events are examined pertaining to the number of errors after a successive number of samples, $T[k]$. Assuming the threshold value, $T[k]$ from Table 14, it is possible to determine the probability of the event where the cumulative error count is greater than $T[k]$ when a wormhole is present, denoted as $P(T[k]^+)$. Additionally, it is possible to determine the probability of the event where the cumulative error count is equal or less than $T[k]$ without a wormhole present, denoted as $P(T[k]^-)$. It is possible to determine the true positive rate, which is the probability of correctly determining if a wormhole is present and is equal to $P(TP) = P(T[k]^+)$. The false-positive rate is the probability detecting a wormhole is present when it is not actually present, calculated by $P(FP) = 1 - P(T[k]^-)$. The results are applied to a BCH(7,4) code and shown in Table 15.

T[k]	k	P(T[k]+)	P(T[k]-)	P(TP)	P(FP)
0.4	1	0.5349	0.8291	0.5349	0.1709
0.7	2	0.7724	0.7134	0.7724	0.2866
1.1	3	0.5554	0.8825	0.5554	0.1175
1.5	4	0.7304	0.8195	0.7304	0.1805
1.8	5	0.8410	0.7572	0.8410	0.2428
3.6	10	0.8656	0.8905	0.8656	0.1095
7.3	20	0.9094	0.9706	0.9094	0.0294
11	30	0.9689	0.9788	0.9689	0.0212
15	40	0.9757	0.9935	0.9757	0.0065
18	50	0.9807	0.9978	0.9807	0.0022

Table 15: BCH(7,4) Wormhole Detection Statistics

Through observation of Table 15 it can be seen that after the first block is received it is possible to accurately predict the presence of a wormhole with a $P(TP) = 44\%$ confidence interval and a false-positive rate of 17%. After 10 samples, or 20 seconds ($N = 7$), this increases to 87% with a false positive rate of 11% and so on. This is visually summarized in Figure 32.

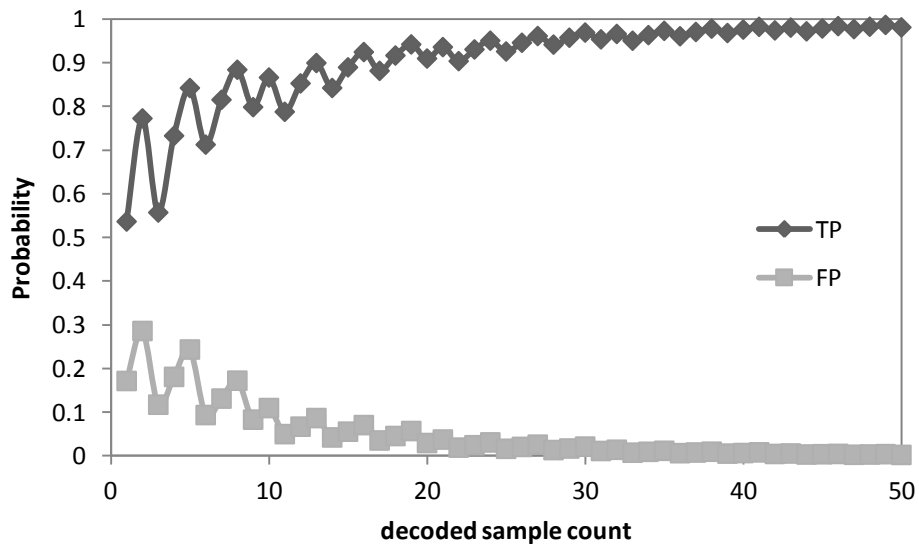


Figure 32: Wormhole Detection Confidence Intervals

It is possible to accomplish similar results at higher code sizes with a tradeoff between the period of time to decode and effective throughput. Choosing the best code is a combination of system design decisions considering the required effective throughput, the accuracy of the model of T_A and the tolerable BER. Future work lies in designing an optimal approach to designing for all the required variables. Other selections of threshold values, T/k , are possible and are left to the system designer, such that a tradeoff between P(TP) and P(FP) is obtained.

A previous method of wormhole detection is discussed in [3] through the use of observed variance of successive values of T_A . However the technique in [3] requires the transmission of a known message in order to measure T_A , meaning that the system cannot simultaneously detect wormholes and send data. The use of error correction codes, introduced in this thesis, allows for the possibility of simultaneous communication and wormhole detection.

6.6 Exata Emulation

As previous sections have focused on a recurring theme using ns2 based simulation, this section presents an OLSR based emulation using the Exata Software [48]. Using the experimental process described in Section 5.4 it is possible to extract a distribution of the unknown jitter values, T_A . In order to add the effects of the Rayleigh distributed wormhole ($\sigma = 0.002s$) as per [5] to successively measured HELLO message traffic a script is used to add the difference of successively received Rayleigh distributed random variables as additional variance simulating the effects of a wormhole. The results are presented in Figure 33.

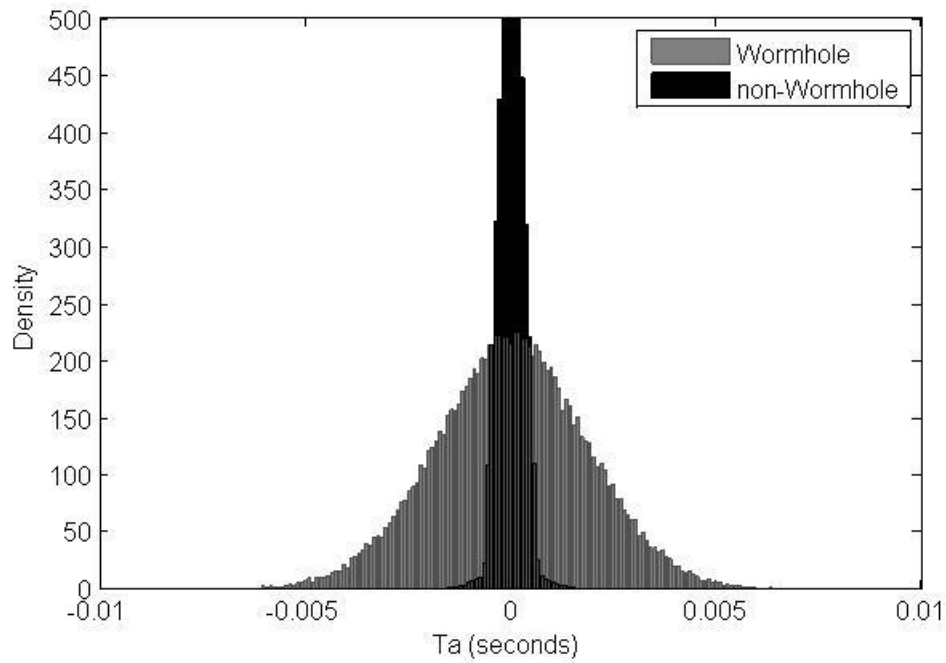


Figure 33: T_A Probability Density Function using Exata

From inspection it is noted that the emulation appears to perform similar to the ns2 simulation shown in Figure 19. There is a clear distinction between the effects on the distribution of T_A in the presence of a wormhole resulting in a distribution approaching the Normal distribution. Using straight binning gives the results presented in Table 16.

N	No Wormhole		Wormhole	
	BER	SER	BER	SER
4	0.0001	0.0002	0.0001	0.0002
5	0.0001	0.0004	0.0002	0.0005
6	0.0002	0.0006	0.0064	0.0380
7	0.0003	0.0014	0.0422	0.2920
8	0.0009	0.0058	0.0888	0.5925
9	0.0053	0.0448	0.1362	0.7876

Table 16: Exata BER and SER using Bins

From a system design perspective it is possible to select the mapping, N , allowing for the required BER or SER that shows a significant increase given the presence of a wormhole. Given a large observable increase in the BER and SER between $N = 8$ and $N = 9$ bits/symbol in Table 16 for the non-wormhole case makes $N = 8$ a good place to apply a coding scheme. Applying a BCH(1023,893) or with $N = 8$ bits code will reduce the observable SER by an order of magnitude to $2.93e-4$.

In summary the Exata emulation model conforms to the expected outcomes and reinforces the results as shown in the previous ns2 simulations. The noted advantage is that Exata emulation is a more realistic environment used to acquire the T_A distribution. One missing factor of the experimental setup is that both emulated nodes are present on the same hardware. Even though they are using their assigned virtual wireless interfaces, which act similar to actual wireless interfaces, the missing aspect is contention for over-the-air transmission of packets. As described in Section 6.1.3, multiple nodes contending for channel or increased channel utilization proportionally increase the variance of T_A .

6.7 OLSRd Test Bed

In order to address the concerns mentioned in the previous section with emphasis of examining the effects of adding propagation over-the-air to an OLSR emulation, an experiment is conducted, as outlined in Section 5.5. In this scenario, OLSRd [51] is installed on two physically separate laptops. As both laptops are trying to compete for channel in contention with other nodes operating in the 802.11 spectrum it is expected that there will be an increase in the variance of T_A . Wormhole traffic noise is added using the modeled difference in Rayleigh distributions as in the case with the Exata emulations from Section 6.6. The results are shown in Figure 34.

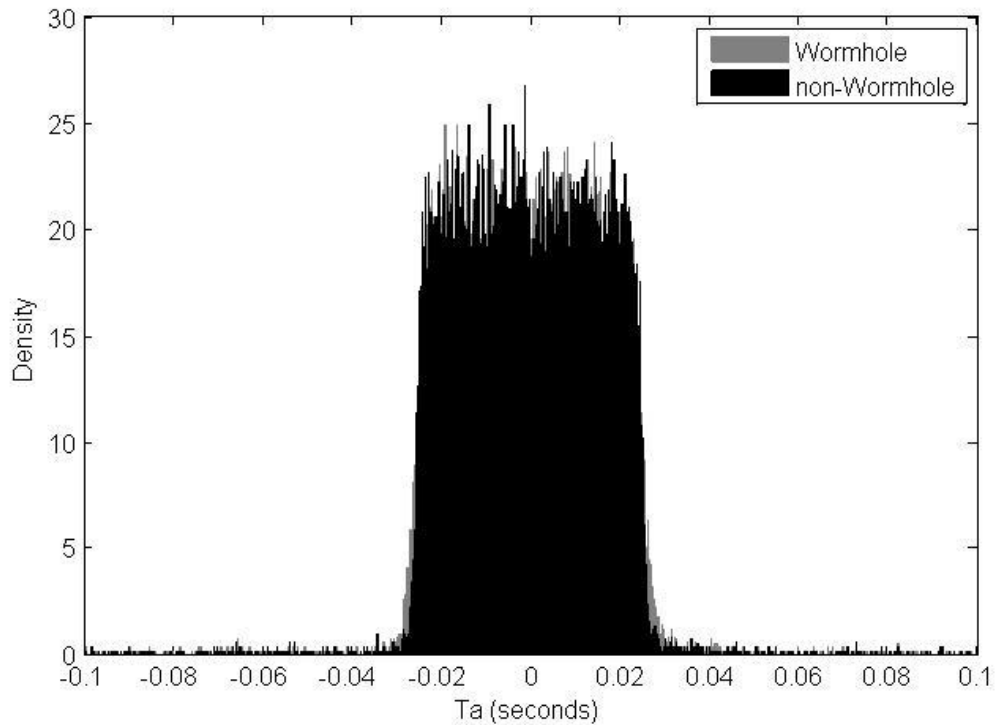


Figure 34: T_A Probability Density Function using OLSRd

This initial result is disappointing as it is not possible to distinguish the effects of the wormhole given the large variance of T_A . Only a small addition can be seen in Figure 34 showing the difference added by the wormhole. This small difference ($3.0e-6$) in variance leads to a large degree of false-positives when predicting wormhole presence. Examining the maximum potential channel capacity, from Equation 16, reveals a severely reduced capacity of 3 bits per period.

The question then becomes if the large variance is a product of the channel contention from CSMA/CA or internal to the configuration of the laptop running OLSRd. A simple experiment is carried out to investigate this. In order to accomplish this one laptop is placed in an environment devoid of 802.11 traffic and consecutive HELLO message traffic is measured at the transmitting interface. This theoretically removes the additional variance associated with channel contention, receiving node stack propagation

delay and operating system overhead. The measured distribution of T_A as measured in a noiseless environment is compared against the distribution of T_A as measured when contending against multiple nodes as shown in Figure 18 to reveal the results in Figure 35.

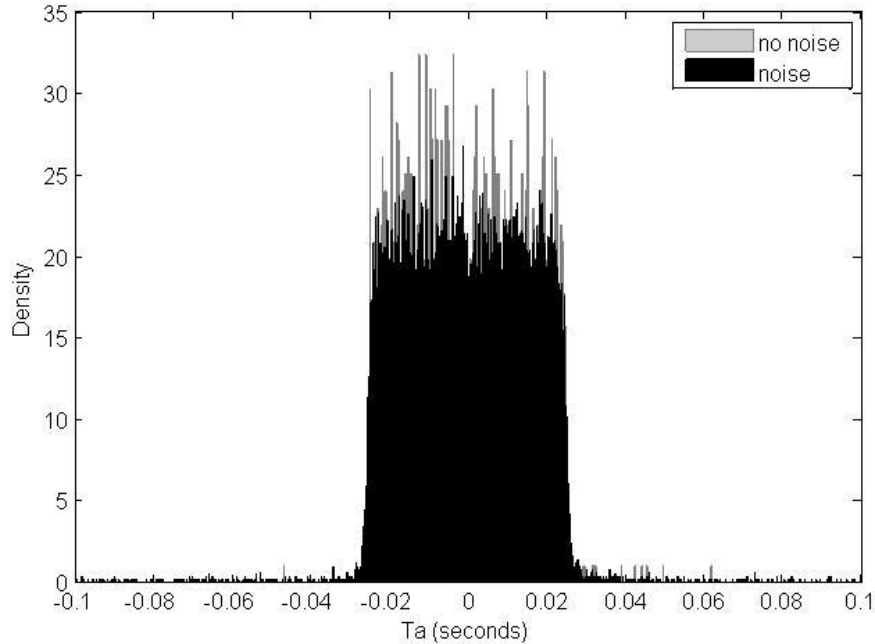


Figure 35: T_A Probability Density Function using OLSRd in Noiseless Environment

The “no noise” distribution represents T_A as measured at the sending interface without the overhead of channel contention as per CSMA/CA. It can be seen from inspection that there is little difference from T_A as measured when transmitting across from node to node as in Figure 34. This adds plausibility to the theory that the greatest source of variance in T_A lay within the transmitting node itself, before the packet reaches the transmitting interface. The conclusion becomes that the implementation of OLSRd as configured on the transmitting node used in the experiments relevant to this section is ineffective. This is in stark comparison to the observed results from the Exata emulation,

which operates similarly to OLSRd in that information is written to an interface for transmission.

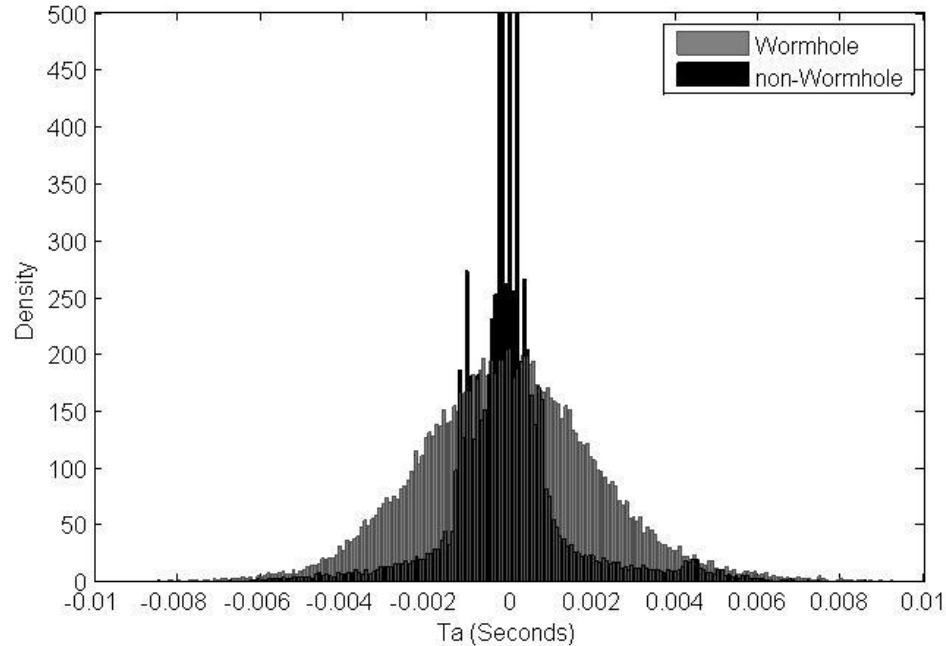


Figure 36: T_A Probability Density Function using Exata and Test-Bed

The proposed solution is to add the missing delay from OLSRd, in terms of transmission and stack propagation delay from the transmitter to the receiver, to the Exata Emulation (which only goes as far as the transmitting wireless interface) for best results. This is possible using the measured delay distribution between the transmitting interface of the OLSRd test-bed and the associated receiver. The results are shown in Figure 36 with additional delay variance added by the Rayleigh distributed wormhole. The results are vastly improved with Equation 16 yielding 7 bits per period as a potential maximum. Computing a table of BER and SER is shown in Table 17.

N	No Wormhole		Wormhole	
	BER	SER	BER	SER
4	0.0038	0.0095	0.0039	0.0108
5	0.0048	0.0138	0.0053	0.0166
6	0.0108	0.0472	0.0180	0.0946
7	0.0187	0.1028	0.0571	0.3597
8	0.0384	0.2199	0.1050	0.6386
9	0.0593	0.3610	0.1503	0.8068

Table 17: Exata and Test-bed BER and SER using Bins

From inspection $N = 6$ bits offers a starting point in terms of BER. Applying forward error correction (FEC) in terms BCH(1023,748) reduces the SER by 2 orders of magnitude to $7.6e-4$. The BER is much lower, than that from [8], as demonstrated in a test-bed environment in the presence of channel contention and realistic noise as seen in Figure 18. The ultimate selection of FEC, through either convolutional coding, linear block coding and symbol encoding will be dependent on the required level of tolerable noise as traded off against throughput which is expected to vary with each unique application.

In summary this chapter has presented an approach towards using error correction coding on a covert channel. A system designer could use a similar approach in measuring T_A and channel capacity and choosing appropriate codes to reduce BER and provide a method of wormhole detection.

7 Chapter: Conclusion

7.1 Summary

This thesis formalizes and improves upon the work from [3] [5], investigating a method of covert communication and wormhole detection using the OLSR ad hoc routing protocol HELLO message traffic. This is accomplished through characterizing the HELLO message covert channel, in Section 3.1, and determining channel noise using the unknown jitter distribution, T_A , explained in Section 3.1. The effects of T_A are first examined theoretically, through their predicted impacts on Shannon's channel capacity limits, in Section 3.2 and 6.1.2. A series of potential improvements to covert channel reliability are introduced through the use of receiver detection theory, as discussed in Section 3.3, and error correction coding mechanisms are examined in Section 3.4 and 6.3. The theory is supported with a series of experiments on the proposed covert channel model, shown in Section 3.5, using: simulation with ns2, emulation with Exata and a test-bed scenario with OLSRd as discussed in Chapter 5. The results are evaluated in Chapter 6 using measurements of error rate and effective throughput. Receiver detection theory mechanisms are independently evaluated and, if effective, combined with other mechanisms, such as error correctional coding, to provide the best potential approach to reducing BER and SER of covert channel traffic while maximizing channel throughput.

The threat of wormholes, as introduced in Chapter 2, are a recurring theme throughout the thesis and are used for test and comparison for all introduced coding mechanisms. Wormhole effects are simulated using a Rayleigh distribution from [16] and added to the measured T_A distributions from experiments detailed further in Chapter 5

and evaluated in Chapter 6. Wormhole detection mechanisms are then applied using error correctional coding to count errors in the covert channel.

7.2 Contributions

This thesis improves the OLSR covert channel model first introduced in [3] [5]. Capacity of the covert channel is derived and it is proved that it can be used to quantitatively detect the presence of a network attack via a wormhole. Channel reliability is improved through the reduction of the observable error rate using receiver detection theory and error correction codes as demonstrated in Section 6.2 and 6.3. Longer codes are required to increase effective throughput compared to the non error corrected case. The optimal code size or scheme used is unique to the situation, but good codes can be found using the methods discussed in Chapter 3 and demonstrated in Chapter 6. Additionally, the characteristics of the covert channel are formalized as applicable to binary traffic and offer quantifiable aspects for higher level system design through the examination of channel capacity and error rate.

The stealth of the covert channel is examined, using tests described in Section 4.1; improvements against the method shown in [5] through the use of additive keyed random jitter are shown, ensuring a uniformly distributed set of jitter values independent of covert message traffic symbol coding. This is demonstrated and evaluated in Section 6.1 to offer resistance to statistical and cryptographic analysis. Also, through the use of keyed random jitter it is possible to secure HELLO message traffic against “replay attacks” as each packet delay is unique, dependent on key stream length.

Lastly, additional mechanisms employable by the receiver to detect wormhole presence, based on observed error rates from error coding are introduced in Section 6.5

with the aim of permitting wormhole detection in the presence of variable SNR from competing nodes in an ad hoc environment.

7.3 Future work

A potential evolution of the work presented here lies in the design of a higher-layer system employing the end point techniques presented in this thesis. Such areas could include introducing cryptographic key distribution, discussed in [8], and revocation mechanisms passed through the covert channel or as a part of the OLSR protocol itself. Testing impacts that mobility and topology have on the covert channel for various scenarios and topologies could be performed and used to refine a higher layer system employing the covert channel. Higher layer function of message retransmission is another possible area of research in the context of throughput restricted covert channels.

As the simulation, emulation and test bed models using in this thesis are simplistic they do not account for larger scale implementations and mobility. Potential future work lay in generating these types of scenarios and well as simulating the dynamic conditions of MANETs to further test the concepts of covert communication and wormhole detection presented in this thesis.

In terms of improving the channel capacity additional codes could be further examined, such as turbo codes and puncturing. Additionally, combining the use of convolutional and block coding schemes together as concatenated codes is an area of potential research.

Areas of potential application of the methodologies discussed in this thesis extend to any such algorithm whereby it is possible to apply similar techniques to any

randomized aspect of the communication protocol and use packet delay timing to send covert traffic.

Bibliography or References

- [1] S. Giordano, *Mobile Ad Hoc Networks*. Wiley Online Library, 2002.
- [2] Y. C. Hu, A. Perrig and D. B. Johnson, "Packet leashes: A defense against wormhole attacks in wireless networks," in *INFOCOM 2003. Twenty-Second Annual Joint Conference of the IEEE Computer and Communications*. IEEE Societies, 2003, pp. 1976-1986 vol. 3.
- [3] D. J. Lynch, "wormhole detection through the manipulation of periodic messages in the OLSR protocol," *Masters Abstracts International*, vol. 46, 2007.
- [4] T. Clausen and P. Jacquet, *Optimized Link State Routing Protocol (OLSR) RFC 3626*, 2003.
- [5] M. A. Gorlatova, M. Kelly, R. Liscano and P. C. Mason, "Enhancing frequency-based wormhole attack detection with novel jitter waveforms," in *Security and Privacy in Communications Networks and the Workshops, 2007. SecureComm 2007. Third International Conference on*, 2007, pp. 304-309.
- [6] C. Murthy and B. Manoj, *Ad Hoc Wireless Networks: Architectures and Protocols*. Prentice Hall PTR, 2004.
- [7] S. Li and A. Epliremidis, "A network layer covert channel in ad-hoc wireless networks," in *Sensor and Ad Hoc Communications and Networks, 2004. IEEE SECON 2004. 2004 First Annual IEEE Communications Society Conference on*, pp. 88-96.
- [8] S. Li, "Covert Channels and Anonymous Communication in Ad-hoc Networks," *Dissertation Abstracts International*, vol. 68, 2007.
- [9] *IEEE Standard for Information Technology-Telecommunications and Information Exchange Between Systems-Local and Metropolitan Area Networks-Specific Requirements - Part 11: Wireless LAN Medium Access Control (MAC) and Physical Layer (PHY) Specifications*, IEEE Std 802. 11-2007 (Revision of IEEE Std 802. 11-1999), 2007.
- [10] L. Hu and D. Evans, "Using directional antennas to prevent wormhole attacks," in *Network and Distributed System Security Symposium (NDSS)*, 2004, pp. 131-141.
- [11] F. Naït-Abdesselam, "Detecting and avoiding wormhole attacks in wireless ad hoc networks," *Communications Magazine, IEEE*, vol. 46, pp. 127-133, 2008.
- [12] L. Qian, N. Song and X. Li, "Detection of wormhole attacks in multi-path routed wireless ad hoc networks: A statistical analysis approach," *Journal of Network and Computer Applications*, vol. 30, pp. 308-330, 2007.

- [13] S. Choi, D. Kim, D. Lee and J. Jung, "WAP: wormhole attack prevention algorithm in mobile ad hoc networks," in *2008 IEEE International Conference on Sensor Networks, Ubiquitous, and Trustworthy Computing*, 2008, pp. 343-348.
- [14] B. Awerbuch, R. Curtmola, D. Holmer, C. Nita-Rotaru and H. Rubens, "ODSBR: An on-demand secure Byzantine resilient routing protocol for wireless ad hoc networks," *ACM Transactions on Information and System Security (TISSEC)*, vol. 10, pp. 1-35, 2008.
- [15] D. Lynch, S. Knight, M. A. Gorlatova, Y. L. Lamont, R. Liscano and P. C. Mason, "Providing Effective Security in Mobile Ad Hoc Networks Without Affecting Bandwidth or Interoperability," Defence Technical Information Center, 2008.
- [16] M. Gorlatova, P. Mason, M. Wang, L. Lamont and R. Liscano, "Detecting wormhole attacks in mobile ad hoc networks through protocol breaking and packet timing analysis," in *Military Communications Conference, 2006. MILCOM 2006.*, pp. 1-7.
- [17] A. A. Pirzada and C. McDonald, "Establishing trust in pure ad-hoc networks," in *Proceedings of the 27th Australasian Conference on Computer Science-Volume 26*, 2004, pp. 54.
- [18] G. Lavanya, C. Kumar and A. R. M. Arokiaraj, "Secured backup routing protocol for ad hoc networks," in *2010 International Conference on Signal Acquisition and Processing*, 2010, pp. 45-50.
- [19] K. G. Poonam and M. Misra, "A Secure Prioritized Trust Based Multi-path Routing Protocol for Ad Hoc Networks," *Recent Trends in Networks and Communications: International Conferences, NeCoM 2010, WiMoN 2010, WeST 2010, Chennai, India, July 23-25, 2010.Proceedings*, vol. 90, pp. 411, 2010.
- [20] R. C. Bose and J. G. Caldwell, "Synchronizable error-correcting codes," *Information and Control*, vol. 10, pp. 616-630, 1967.
- [21] J. Levy, "Self-synchronizing codes derived from binary cyclic codes," *Information Theory, IEEE Transactions on*, vol. 12, pp. 286-290, 1966.
- [22] V. I. Levenshtein, "Binary codes capable of correcting deletions, insertions, and reversals," *Soviet Physics Doklady*, vol. 10, pp. 707-710, 1966.
- [23] C. E. Shannon, "A mathematical theory of communication," *ACM SIGMOBILE Mobile Computing and Communications Review*, vol. 5, pp. 3-55, 2001.
- [24] J. K. Millen, "Finite-state noiseless covert channels," in *Computer Security Foundations Workshop II, 1989., Proceedings of the*, 1989, pp. 81-86.

- [25] I. S. Moskowitz and A. R. Miller, "Simple timing channels," in *Research in Security and Privacy, 1994. Proceedings., 1994 IEEE Computer Society Symposium on*, 1994, pp. 56-64.
- [26] B. R. Venkatraman and R. E. Newman-Wolfe, "Capacity estimation and auditability of network covert channels," in *Security and Privacy, 1995. Proceedings., 1995 IEEE Symposium on*, 1995, pp. 186-198.
- [27] C. E. Shannon and W. Weaver, *The Mathematical Theory of Communication*. Citeseer, 1959.
- [28] L. Van Den Doel, A. Klein, S. Ellenberger, H. Netten, F. Boddeke, L. Van Vliet and I. Young, "Quantitative evaluation of light microscopes based on image processing techniques," *Bioimaging*, vol. 6, pp. 138-149, 1998.
- [29] F. GRAY, "Pulse code communication," US Patent 2,632,058, 1953.
- [30] B. P. Lathi, *Modern Digital and Analog Communication Systems*. Oxford University Press, Inc. New York, NY, USA, 1995.
- [31] P. Elias, "Coding for noisy channels," *IRE Conv.Rec*, vol. 4, pp. 37-46, 1955.
- [32] A. J. Viterbi, "An intuitive justification and a simplified implementation of the MAP decoder for convolutional codes," *Selected Areas in Communications, IEEE Journal on*, vol. 16, pp. 260-264, 1998.
- [33] S. Gianvecchio and H. Wang, "Detecting covert timing channels: An entropy-based approach," in *Proceedings of the 14th ACM Conference on Computer and Communications Security*, 2007, pp. 307-316.
- [34] S. Cabuk, C. E. Brodley and C. Shields, "IP covert timing channels: Design and detection," in *Proceedings of the 11th ACM Conference on Computer and Communications Security*, 2004, pp. 178-187.
- [35] B. Hechenleitner and K. Entacher, "On shortcomings of the ns-2 random number generator," in *Proceedings of the Communication Networks and Distributed Systems Modeling and Simulation*, 2002, .
- [36] A. Francillon and C. Castelluccia, "TinyRNG: A cryptographic random number generator for wireless sensors network nodes," in *Modeling and Optimization in Mobile, Ad Hoc and Wireless Networks and Workshops, 2007. WiOpt 2007. 5th International Symposium on*, 2007, pp. 1-7.
- [37] L. Frikha, Z. Trabelsi and W. El-Hajj, "Implementation of a covert channel in the 802.11 header," in *Wireless Communications and Mobile Computing Conference, 2008. IWCMC'08. International*, 2008, pp. 594-599.

- [38] S. Zander, G. Armitage and P. Branch, "A survey of covert channels and countermeasures in computer network protocols," *IEEE Communications Surveys & Tutorials*, 3rd Quarter, vol. 9, pp. 44-57, 2007.
- [39] G. Liu, J. Zhai, Y. Dai and Z. Wang, "Covert timing channel with distribution matching," in *2009 International Conference on Multimedia Information Networking and Security*, 2009, pp. 565-568.
- [40] S. Azad, A. Rahman and F. Anwar, "A performance comparison of proactive and reactive routing protocols of Mobile Ad-hoc Network (MANET)," *Journal of Engineering and Applied Sciences*, vol. 2, pp. 891-896, 2007.
- [41] S. Gowrishankar, T. Basavaraju, M. Singh and S. K. Sarkar, "Scenario based performance analysis of AODV and OLSR in mobile ad hoc networks," in *Proceedings of the 24th South East Asia Regional Computer Conference*, 2007, pp. 18-19.
- [42] D. Nguyen and P. Minet, "Interference effects on the OLSR protocol: Ns-2 simulation results," in *Third Annual Mediterranean Ad Hoc Networking Workshop, June 2004, Bodrum Turkey*, .
- [43] M. H. Manshaei, G. R. Cantieni, C. Barakat and T. Turletti, "Performance analysis of the IEEE 802.11 MAC and physical layer protocol," in *Proceedings of the Sixth IEEE International Symposium on World of Wireless Mobile and Multimedia Networks*, 2005, pp. 88-97.
- [44] E. Haghani, M. N. Krishnan and A. Zakhori, "A Method for Estimating Access Delay Distribution in IEEE 802.11 Networks," in *Global Telecommunications Conference (GLOBECOM 2011), 2011 IEEE*, 2011, pp. 1-6.
- [45] S. Ivanov, A. Herms and G. Lukas, "Experimental validation of the ns-2 wireless model using simulation, emulation, and real network," in *Communication in Distributed Systems (KiVS), 2007 ITG-GI Conference*, 2007, pp. 1-12.
- [46] F. Haq and T. Kunz, "Simulation vs. emulation: Evaluating mobile ad hoc network routing protocols," in *Proceedings of the International Workshop on Wireless Ad-Hoc Networks (IWWAN 2005)*, 2005, .
- [47] J. Hortelano, M. Nácher, J. C. Cano, C. Calafate and P. Manzoni, "Evaluating the goodness of MANETs performance results obtained with the ns-2 simulator," in *Proceedings of the 2nd International Conference on Performance Evaluation Methodologies and Tools*, 2007, pp. 1-7.
- [48] R. Bagrodia, "Accelerating Wireless Device Development with Network Emulation," [Online] Available: www.Scalable-Networks.com/pdf/MPD_finalproof.Pdf.

- [49] S. Seth and A. Gankotiya, "Emulating wormhole attack under wireless mesh network," in *Proceedings of the International Conference on Information Science and Applications ICISA 2010*, Chennai, India, 2010, .
- [50] T. Clausen, C. Dearlove and P. Jacquet, "The optimized link state routing protocol version 2, IETF, draft-ietf-manet-olsrv2-11," 2010.
- [51] A. Tønnesen, "Implementing and extending the optimized link state routing protocol," *Master's Thesis. University of Oslo, Norway*, 2004.
- [52] M. Ikeda, L. Barolli, G. De Marco, T. Yang and A. Durresi, "Experimental and simulation evaluation of OLSR protocol for mobile ad-hoc networks," *Network-Based Information Systems*, pp. 111-121, 2008.
- [53] A. M. Y. Bigloo, T. A. Gulliver and V. K. Bhargava, "Maximum-likelihood decoding and code combining for DS/SSMA slotted ALOHA," *Communications, IEEE Transactions on*, vol. 45, pp. 1602-1612, 1997.
- [54] K. Islam, P. Rabiei, S. Dusad, N. Al-Dhahir, S. Diggavi and A. Calderbank, "Linear Diversity-Embedding STBC: Systems Issues and Applications," to appear *IEEE Transactions on Communications*, 2008.
- [55] R. H. Morelos-Zaragoza and J. Wiley, Eds., *The Art of Error Correcting Coding*. Wiley Online Library, 2002.
- [56] T. K. Moon, *Error Correction Coding: Mathematical Methods and Algorithms*. Wiley-Blackwell, 2005.